

This manuscript version is distributed under the CC-BY-NC-ND (Creative Commons) license.

It has appeared in final form as:

Van Albada SJ, Robinson PA. Mean-field modeling of the basal ganglia-thalamocortical system. I. Firing rates in healthy and parkinsonian states (2009) *J Theor Biol* 257: 642–663, DOI: 10.1016/j.jtbi.2008.12.018

arXiv:1801.01822v1 [q-bio.NC] 5 Jan 2018

# Mean-field modeling of the basal ganglia-thalamocortical system. I. Firing rates in healthy and parkinsonian states

S. J. van Albada<sup>a,b</sup>

P. A. Robinson<sup>a,b,c</sup>

January 8, 2018

<sup>a</sup>School of Physics, The University of Sydney  
New South Wales 2006, Australia

<sup>b</sup>The Brain Dynamics Centre, Westmead Millennium Institute  
Westmead Hospital and Western Clinical School of the University of Sydney  
Westmead, New South Wales 2145, Australia

<sup>c</sup>Faculty of Medicine, The University of Sydney  
New South Wales 2006, Australia

## Abstract

Parkinsonism leads to various electrophysiological changes in the basal ganglia-thalamocortical system (BGTCS), often including elevated discharge rates of the subthalamic nucleus (STN) and the output nuclei, and reduced activity of the globus pallidus external segment (GPe). These rate changes have been explained qualitatively in terms of the direct/indirect pathway model, involving projections of distinct striatal populations to the output nuclei and GPe. Although these populations partly overlap, evidence suggests dopamine depletion differentially affects cortico-striato-pallidal connection strengths to the two pallidal segments. Dopamine loss may also decrease the striatal signal-to-noise ratio, reducing both cortico-striatal coupling and striatal firing thresholds. Additionally, nigrostriatal degeneration may cause secondary changes including weakened lateral inhibition in the GPe, and mesocortical dopamine loss may decrease intracortical excitation and especially inhibition. Here a mean-field model of the BGTCS is presented with structure and parameter estimates closely based on physiology and anatomy. Changes in model rates due to the possible effects of dopamine loss listed above are compared with experiment. Our results suggest that a stronger indirect pathway, possibly combined with a weakened direct pathway, is compatible with empirical evidence. However, altered corticostriatal connection strengths are probably not solely responsible for substantially increased STN activity often found. A lower STN firing threshold, weaker intracortical inhibition, and stronger striato-GPe inhibition help explain the relatively large increase in STN rate. Reduced GPe-GPe inhibition and a lower GPe firing threshold can account for the comparatively small decrease in GPe rate frequently observed. Changes in cortex, GPe, and STN help normalize the cortical rate, also in accord with experiments. The model integrates the basal ganglia into a unified framework along with an existing thalamocortical model that already accounts for a wide range of electrophysiological phenomena. A companion paper discusses the dynamics and oscillations of this combined system.

## 1 Introduction

The basal ganglia have been studied extensively in connection with a variety of motor and cognitive disorders, including Parkinson's disease (PD), Huntington's disease, and schizophrenia (Bar-Gad et al., 2003; Goldman-Rakic and Selemon, 1990; Gray et al., 1991; Graybiel, 1990; Haber and Gdowski, 2004; Swerdlow and Koob, 1987; Walters et al., 2007; Waters et al., 1988). In PD, degeneration of dopaminergic neurons in the substantia nigra pars compacta (SNc) leads to changes in tonic and phasic neuronal discharges in the components of the basal ganglia-thalamocortical system (BGTCS). Many studies have provided detailed descriptions of changes in discharge patterns with parkinsonism, as well as suggestions for the pathways and mechanisms by which these patterns arise (Bar-Gad et al., 2003; Bergman and Deuschl, 2002). An influential

proposal is the direct/indirect pathway model of Albin et al. (1989), which postulates distinct pathways through two populations of striatal neurons expressing either the D1 class or D2 class of dopamine receptor. D1-expressing neurons project monosynaptically to the globus pallidus internal segment (GPi) and the substantia nigra pars reticulata (SNr), giving rise to the *direct pathway*, whereas D2-expressing neurons project polysynaptically to these output nuclei via the globus pallidus external segment (GPe) and the subthalamic nucleus (STN), forming the *indirect pathway*. By enhancing transmission through D2 cells and reducing transmission through D1 cells, degeneration of nigrostriatal dopaminergic neurons would decrease the GPe firing rate in this model, and increase the rates of STN and the output nuclei. This would amplify the inhibitory effect exerted by the output nuclei on the thalamus, leading to parkinsonian symptoms such as akinesia and tremor. The direct/indirect pathway model was later modified to include the so-called *hyperdirect pathway*, upon the realization that the STN receives input directly from the cortex, forming another major input station of the basal ganglia (Nambu et al., 2000). The direct, indirect, and hyperdirect pathways are illustrated in Figure 1.

Physiologically-based mathematical models allow electrophysiological phenomena to be studied not just qualitatively but also in quantitative terms, thus better clarifying the underlying mechanisms. Most computational studies of the basal ganglia consider networks of neurons. Terman et al. (2002) presented a model of the network formed by the STN and the GPe, which displayed either  $<1$  Hz or 4–6 Hz oscillations upon dopamine depletion, depending on the network architecture and connection strengths. Rubin and Terman (2004) described a neuronal network model that included also the GPi and the thalamus, and illustrated how high-frequency stimulation of the STN may facilitate signal transmission by the thalamus in parkinsonian patients. Specific aspects of basal ganglia function, such as visual attention (Jackson et al., 1994) and decision threshold tuning (Lo and Wang, 2006) have also been addressed in computational studies. Leblois et al. (2006) presented a neuronal network model that could account for loss of action selection and predicted the appearance of  $\sim 7$ –10 Hz oscillations in the hyperdirect loop after dopamine depletion. In a detailed model building on earlier work (Gurney et al., 2001a,b; Humphries and Gurney, 2001), Humphries et al. (2006) reproduced the enhanced  $\sim 1$  Hz activity that is observed in the STN and globus pallidus (GP; the rodent homolog of the GPe) of anesthetized rats with nigrostriatal lesions, and gamma-band activity in the healthy state.

The purpose of this paper is to describe a physiologically plausible mean-field model of the intact BGTCS that can reproduce firing rates characteristic of PD with realistic changes in parameters relative to the non-parkinsonian case. A mean-field model has the advantage over neuronal network models that it can predict large-scale properties of neuronal assemblies and directly assess their dependence on connection strengths between populations. Moreover, mean-field models have comparatively few parameters, and can be implemented for a larger number of populations and connections without leading to an overly complicated set of equations or excessive computational demands. Thus, both numerical and analytical results are more readily obtained. An existing mean-field model has been used successfully to describe thalamocortical oscillations contributing to the electroencephalogram (EEG), yielding predictions of cortical frequency and wavenumber spectra (O’Connor et al., 2002; Robinson et al., 2001a), coherence and correlations (Robinson, 2003), the electrophysiology of epileptic seizures (Breakspear et al., 2006; Robinson et al., 2002), evoked response potentials and steady-state evoked potentials (Kerr et al., 2008; Robinson et al., 2001b), and changes with arousal (Robinson et al., 2005). This study provides a first step towards integrating the thalamocortical system and the basal ganglia in a unified framework.

Our model adds to existing models by estimating the strengths of a large number of connections in the BGTCS, and investigating the dependence of average firing rates on these connection strengths. The influences of various projections not present in the classic direct/indirect pathway model are explored, and possible reasons for the prominent hyperactivity of the STN in parkinsonism are discussed. Estimates of parameters and firing rates are based on an extensive review of the experimental literature. Changes in firing rates with nigrostriatal dopaminergic denervation are an aspect of the electrophysiology of the BGTCS that remains to be explained quantitatively, and as such are of key scientific interest. Moreover, steady states form an essential basis for the analysis of dynamics and oscillations, which are the subject of a companion paper [Van Albada et al. (2009); henceforth referred to as Paper II].

It is almost impossible for a model of a system as complex as the basal ganglia to incorporate

all relevant data, especially as new discoveries are regularly being made. Thus we attempt to distill the main findings from the wealth of available data, while providing a framework that allows for more detailed modeling of basal ganglia structure, activity, and function in future.

The physiological background of our model is presented in Sec. 2. Section 3 details the model equations and the possible effects of dopamine depletion. The model is then used to derive firing rates of the BGTCS in the normal and parkinsonian states in Sec. 4. As mentioned above, these results lay the foundation for the analysis of dynamics and oscillations in Paper II.

## 2 Physiological background

This section describes the physiological background of the BGTCS on which our model is based, which allows us to compare the predictions of our model with experimental results. Section 2.1 details the main functional connections between the basal ganglia nuclei, its thalamic projection sites, and the cerebral cortex. Section 2.2 is devoted to the firing rates of the various components in the normal state and in PD.

### 2.1 Functional connectivity of the basal ganglia

The main structures comprising the basal ganglia are the striatum (caudate nucleus, putamen, and ventral striatum), pallidum (internal and external segments and ventral pallidum), substantia nigra (pars compacta, pars reticularis, and pars lateralis), and subthalamic nucleus. They are part of a system of pathways, some of which form closed loops, connecting the basal ganglia with the cerebral cortex and thalamus. Information flow through the basal ganglia has been described as following three parallel, mostly separate, pathways (sensorimotor, association, and limbic), which may be further subdivided into somatotopically organized pathways or pathways concerned with different aspects of motor function and cognition (Alexander et al., 1986; Alexander and Crutcher, 1990). The main functional connections of the BGTCS are depicted in Fig. 1.

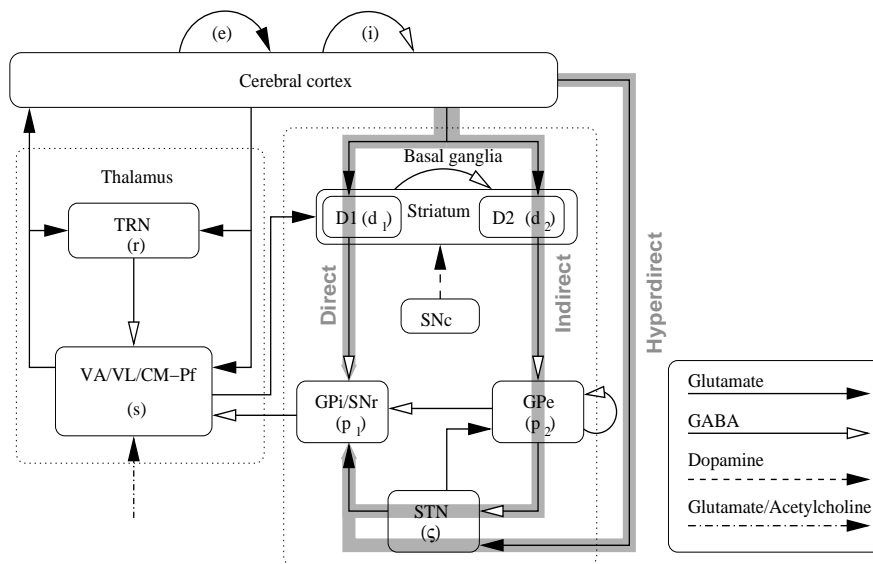


Figure 1: Major functional connections of the BGTCS. External input reaches the thalamus primarily from the brainstem. Filled arrowheads represent excitatory projections, open arrowheads inhibitory ones. Subscripts corresponding to each component are given in parentheses, and gray arrows indicate the direct, indirect, and hyperdirect pathways.

The SNc and its medial extension, the ventral tegmental area (VTA), send important dopaminergic projections to the striatum (Gerfen, 1992; Haber et al., 2000; Hanley and Bolam, 1997). Excitatory input from the cortex also reaches the basal ganglia mainly at the striatum; sensorimotor inputs terminate more specifically in the putamen, which also receives some associative

input (Percheron et al., 1984). The striatum is organized into ‘patch’ and ‘matrix’ compartments, which are distinguished on the basis of biochemical markers and their detailed sources and targets of activity (Gerfen et al., 1987). More than 90% of striatal neurons are medium spiny neurons (Yelnik et al., 1991), which can be classified both according to their compartmental origin and the class of dopamine receptor they primarily express (D1 or D2). These classifications are partly overlapping: both patch and matrix contain D1 and D2 receptors, although relative receptor densities may differ between compartments (Joyce et al., 1988). Neurons with D1-type receptors coexpress the peptides dynorphin and substance P; D2 cells are enriched in enkephalin (Gerfen et al., 1990). According to the classic direct and indirect pathway model (Albin et al., 1989; Alexander and Crutcher, 1990), D1 neurons project primarily to the output nuclei GPi and SNr, whereas D2 neurons project primarily to the GPe. Striatal impulses exert an overall excitatory effect on the thalamus and cortex via the direct pathway from the striatum to the output nuclei, and an inhibitory effect via the indirect pathway to the output nuclei via the GPe and the STN (cf. Fig. 1).

In the direct/indirect pathway model, the SNc would mainly facilitate corticostriatal transmission to D1 cells and inhibit transmission to D2 cells, so that dopamine loss would favor the indirect pathway. This simplified view has been called into question by findings that the segregation between D1 and D2 receptors is incomplete (Aizman et al., 2000; Inase et al., 1997; Surmeier et al., 1992, 1996), and that neurons expressing both receptor types project to both pallidal segments (Lévesque and Parent, 2005; Nadjar et al., 2006; Wu et al., 2000). The extent of colocalization of D1 and D2 class receptors reported in the literature ranges from almost none (Hersch et al., 1995; Le Moine and Bloch, 1995), to 20–35% (Inase et al., 1997; Lester et al., 1993; Meador-Woodruff et al., 1991), about half (Surmeier et al., 1996), or nearly all medium spiny neurons (Aizman et al., 2000). Some of these discrepancies may be explained by a lack of sensitivity of *in situ* hybridization techniques to low levels of mRNA, which are detected after mRNA amplification (Le Moine and Bloch, 1995), suggesting that even in cells where these receptors occur together, one type usually predominates. Therefore we assume that a significant proportion of striatal neurons expresses a large majority of either D1 or D2 class dopamine receptors.

Despite the collateralization of striatofugal axons, many studies have also shown that projections in the direct and indirect pathways can be at least partly distinguished. In a rat model of PD, striatopallidal neurons show increased expression of mRNA encoding D2 receptors and enkephalin, whereas striatonigral neurons show a reduction in mRNA for D1 receptors and substance P (Gerfen et al., 1990). In Huntington’s disease the striatal projection to GPe is more vulnerable than that to GPi (Deng et al., 2004; Reiner et al., 1988; Walker, 2007). In a study of mouse brain slices, Day et al. (2006) found that lack of dopamine causes a profound loss of dendritic spines on striatopallidal neurons but not on striatonigral neurons. Thus, we assume a partial segregation of the projections to the output nuclei and the GPe. However, our model provides an overarching framework in which both possibilities (segregation or overlap) can be incorporated, and differences between these possibilities can be explored.

Besides medium spiny neurons, the striatum contains various types of interneurons, including cholinergic tonically active neurons that make up about 1–5% of the striatum (Aosaki et al., 1995; Kawaguchi et al., 1995; Kimura et al., 1984), and GABAergic inhibitory interneurons that make up only a small percentage of the striatal population but have strong effects (Bolam et al., 2000; Koós and Tepper, 1999). In addition, medium spiny neurons have local axon collaterals through which GABA exerts a depolarizing effect at rest, but a hyperpolarizing effect near spike threshold (Plenz, 2003; Taverna et al., 2004). Thus, lateral connections between medium spiny neurons will moderate the striatal firing rate with strong cortical inputs.

In primates the SNr and GPi are part of separate circuits, with different target areas and sources of activity (Ilinsky et al., 1993). The SNr receives input mostly from the caudate nucleus, which relays associative information from the prefrontal cortex as well as inputs from the frontal eye fields. It sends GABAergic projections mainly to the magnocellular part of the ventral anterior nucleus (VAmc) of the thalamus and is involved in the control of eye movements (Parent and Hazrati, 1995). The GPi, on the other hand, receives input mainly from the premotor and primary motor cortices via the putamen, and relays this mainly to the ventrolateral thalamic nucleus (VL) (Haber and Gdowski, 2004). Despite these differences, GPi and SNr are often modeled as a single structure due to their closely related inputs and outputs, as well as

similarities in cytology and function (Alexander and Crutcher, 1990; Bar-Gad et al., 2003). Since electrophysiological studies of the remaining basal ganglia nuclei often do not distinguish between associative and sensorimotor territories, it is difficult in practice to differentiate between the inputs to GPi and SNr. We therefore model these nuclei as a single combined structure, although the response to dopaminergic cell loss is more pronounced in the GPi (Mitchell et al., 1986; Wichmann et al., 1999).

Apart from the ventral anterior nucleus (VA) and VL, target sites of the basal ganglia output nuclei have been identified in the centromedian-parafascicular complex (CM-Pf) (Kim et al., 1976; Parent et al., 2001). Neurons in VA, VL, and CM-Pf send axons back mainly to the matrix compartment of the striatum (Carpenter, 1981; Gonzalo et al., 2002; McFarland and Haber, 2000; Parent, 1990; Ragsdale and Graybiel, 1988; Sadikot et al., 1992). Studies suggest that the influence of these projections is excitatory (Haber and Gdowski, 2004; Sadikot et al., 1992).

The GPe sends an important inhibitory projection to the STN, which in turn excites both the GPe and the output nuclei (Hamada and DeLong, 1992; Kita et al., 1983; Parent and Hazrati, 1995; Shink et al., 1996). However, the pattern of connections between GPe, GPi, and STN is complicated by a direct projection from approximately a third of GPe neurons forming synapses on GPi cell bodies or proximal dendrites (Hazrati et al., 1990; Sato et al., 2000; Shink and Smith, 1995; Smith et al., 1994). These projections derive from axons also branching to STN and sometimes SNr (Sato et al., 2000). Besides its substantial innervation by striatum and STN, the GPe is extensively connected via local axon collaterals, which may exert a strong inhibitory influence since they terminate on cell bodies and proximal dendrites (Kita, 1994; Nambu and Llinás, 1997; Ogura and Kita, 2000).

As discussed in the Introduction, the STN forms an additional input station of the basal ganglia. The cortico-STN projection originates in the primary motor cortex (M1) and somatosensory and premotor cortices, including the supplementary motor area (SMA) (Afsharpour, 1985; Nambu et al., 1996, 1997, 2000; Parent and Hazrati, 1995). Because the STN influences the thalamus mainly via direct projections to the GABAergic output nuclei, the overall effect of this pathway on thalamic targets is inhibitory.

Connections within and between the thalamus and cortex complete the basal ganglia-thalamocortical system. These connections follow a previous model of brain electrical activity involving only the thalamus and cortex (Rennie et al., 1999; Robinson et al., 1997, 2001a, 2003a, 2005). The thalamic reticular nucleus (TRN) exerts a powerful inhibitory effect over the relay nuclei, from which it receives excitatory input. Both TRN and the relay nuclei are densely innervated by glutamatergic cortical neurons. Within the cortex our model includes excitatory corticocortical and inhibitory local circuit neurons. Finally, sensory stimuli reaching the thalamus mainly from the brainstem are modeled as external input.

## 2.2 Data on firing rates in normal and parkinsonian states

This section provides a summary of the mean firing rates of the basal ganglia nuclei and their thalamic and cortical targets in the normal and parkinsonian states, for comparison with modeling results in Sec. 4.

Some studies of firing rates and patterns of basal ganglia are performed during stereotaxic surgery for PD. However, most studies use one of two well-known animal models of parkinsonism. In monkeys, symptoms most closely resembling human parkinsonism are obtained by lesioning nigrostriatal neurons using 1-methyl-4-phenyl-1,2,3,6-tetrahydropyridine (MPTP) (DeLong, 1990). Depending on the species, this can lead to akinesia, bradykinesia, and/or resting tremor at frequencies of 4–8 Hz. Another widely used paradigm is the 6-hydroxydopamine (6-OHDA) rodent model of PD (Ungerstedt, 1968).

The average discharge rate of neurons in the primary motor and somatosensory cortices of monkeys is about 5–20 s<sup>-1</sup> depending on the level of activity (Wannier et al., 1991). Some studies found the cortical rate to be unchanged with MPTP- or 6-OHDA-induced parkinsonism (Dejean et al., 2008; Goldberg et al., 2002), and parkinsonian symptoms have instead been linked with abnormal temporal organization of motor cortical activity (Brown, 2000; Goldberg et al., 2002; Salenius et al., 2002). On the other hand, fMRI studies in PD patients have found impaired activation of cortical areas normally co-activated with the striatum (Monchi et al., 2004, 2007),

and a PET study showed that blood flow in the SMA of PD patients during performance of a motor task is reduced relative to healthy subjects (Jenkins et al., 1992).

Most striatal medium spiny neurons fire spontaneously at a low rate of  $0.5\text{--}2\text{ s}^{-1}$  (DeLong et al., 1983; Haber and Gdowski, 2004; Kimura et al., 1996). However, Kiyatkin and Rebec (1999) reported a highly skewed distribution of striatal firing rates in awake rats, with a small fraction of fast-spiking neurons taking the average rate up to  $\sim 6\text{ s}^{-1}$ . This matches the rate in monkeys recorded by Goldberg et al. (2002). Several studies in 6-OHDA-lesioned rats have revealed elevated activity in striatal neurons with respect to healthy rats (Chen et al., 2001; Kish et al., 1999; Tseng et al., 2001; Walters et al., 2007), which may be due to a large activity increase in striatopallidal neurons and a smaller activity decrease in striatonigral neurons (Mallet et al., 2006). A relatively high average firing rate of  $\sim 10\text{ s}^{-1}$  was also recorded in the putamen of PD patients (Magnin et al., 2000). On the other hand, one study reported the discharge rate of caudate neurons to be decreased from  $\sim 6\text{ s}^{-1}$  to  $\sim 4\text{ s}^{-1}$  with MPTP lesion (Yoshida, 1991), while another study found no change (Goldberg et al., 2002).

The normal GPi firing rate in primates is in the range  $60\text{--}90\text{ s}^{-1}$ , with an increase of about  $10\text{--}20\text{ s}^{-1}$  after MPTP treatment in monkeys (Filion and Tremblay, 1991; Heimer et al., 2002; Yoshida, 1991). In line with these results, normalization of dopamine levels by application of the dopamine agonist apomorphine decreases the average firing rate of GPi neurons in PD patients (Merello et al., 1999). On the other hand, some studies found no significant change in average firing rates of GPi (Bergman et al., 1994; Wichmann et al., 1999) or its rodent homolog, the entopeduncular nucleus (EP) (Robledo and Feger, 1991). In one study the mean discharge frequency of GPi neurons in PD patients was only  $\sim 59\text{ s}^{-1}$  (Sterio et al., 1994), and another study (Hutchison et al., 1994) found the average firing rate of GPi neurons in PD patients to be  $67\text{ s}^{-1}$  and no different from the average rate reported for normal monkeys. However, the posteroventral portion of the GPi showed increased activity (mean rate  $82\text{ s}^{-1}$ ). This suggests that dopamine loss increases the firing rate in the sensorimotor portion of the GPi, while other parts are relatively unaffected. Magnin et al. (2000) similarly differentiated between the GPi as a whole, which had a firing rate of  $91\text{ s}^{-1}$  in PD patients, and the internal part of the GPi, which discharged at  $114\text{ s}^{-1}$ .

SNr neurons in normal monkeys discharge at a mean rate comparable to that of GPi neurons ( $50\text{--}70\text{ s}^{-1}$ ) (DeLong et al., 1983; Schultz, 1986). However, the SNr is less affected by dopamine lesions than other nuclei. For instance, the mean firing rate of SNr neurons in PD patients is  $\sim 71\text{ s}^{-1}$  (Hutchison et al., 1998), very close to that in normal monkeys. In a study by Walters et al. (2007), SNr neurons of 6-OHDA-lesioned rats displayed a non-significant decrease in average firing rate 7–10 days post-lesion. MacLeod et al. (1990) measured a short-term decrease ( $< 10$  days postlesion) in the average firing rate of SNr neurons upon treatment with 6-OHDA, but the firing rate had normalized after a period of  $> 6$  months. On the other hand, Benazzouz et al. (2000) and Burbaud et al. (1995) recorded significantly elevated discharge rates in the SNr of rats several weeks after lesions of the SNc. Alterations in SNr firing rates and patterns reported by Wichmann et al. (1999) were less pronounced than those in the GPi, and no significant change in SNr firing rate was observed.

GPe neurons can be divided into two main categories based on firing characteristics (DeLong, 1971; Filion and Tremblay, 1991; Sterio et al., 1994): about 85% of GPe neurons display high-frequency bursts of activity interspersed with long intervals of silence lasting up to several seconds. These neurons have a mean firing rate of  $\sim 55\text{ s}^{-1}$ . The remaining 15% are slowly discharging neurons with occasional bursts and an average rate of  $\sim 10\text{ s}^{-1}$ . Conflicting reports exist concerning changes in GPe rate, some studies finding a decrease of about  $10\text{--}20\text{ s}^{-1}$  with nigrostriatal lesions (Boraud et al., 1998; Filion and Tremblay, 1991; Heimer et al., 2002; Pan and Walters, 1988), whereas others detected no significant change (Goldberg et al., 2002; Hutchison et al., 1994; Magill et al., 2001; Walters et al., 2007). Average GPe firing rates of  $40\text{--}60\text{ s}^{-1}$  have been reported in patients with medication-resistant PD (Hutchison et al., 1994; Magnin et al., 2000; Sterio et al., 1994).

STN cells in monkeys display spontaneous tonic activity, firing at approximately  $20\text{--}30\text{ s}^{-1}$ , often in pairs or triplets of spikes (DeLong et al., 1985; Georgopoulos et al., 1983). Dopaminergic lesion has been reported to increase this rate by  $\sim 7\text{ s}^{-1}$  (Bergman et al., 1994). In agreement with these findings, STN neurons of PD patients have relatively high discharge rates of  $37\text{--}43$

$\text{s}^{-1}$  (Benazzouz et al., 2002; Hutchison et al., 1998), while Levy et al. (2000) measured a higher median firing rate in STN cells that displayed tremor-related activity ( $53 \text{ s}^{-1}$ ) than in non-tremor-related cells ( $43 \text{ s}^{-1}$ ) of PD patients. Increases of  $4\text{--}6 \text{ s}^{-1}$  in mean STN discharge rate have been observed in 6-OHDA-treated rats (Kreiss et al., 1997; Walters et al., 2007), although some studies found no change or even a reduction in firing rate up to 4 weeks postlesion (Hollerman and Grace, 1992; Ni et al., 2001a).

Firing in pallidal-receiving areas of the thalamus was found to be  $7\text{--}8 \text{ s}^{-1}$  in PD patients compared with  $18\text{--}19 \text{ s}^{-1}$  in patients with essential tremor or pain (Molnar et al., 2005). Since the basal ganglia are not thought to be involved in the pathophysiology of pain or essential tremor, a rate of  $18\text{--}19 \text{ s}^{-1}$  probably represents normal thalamic activity, suggesting that activity of pallidal-receiving thalamic areas is reduced in PD. A significant decrease in thalamic activity was found in MPTP-treated cats (Schneider and Rothblat, 1996) but not monkeys (Pessiglione et al., 2005). However, metabolic studies in 6-OHDA-treated rats and MPTP-treated monkeys strongly point to hypoactivity of basal ganglia-receiving areas of the thalamus in parkinsonism (Gnanalingham et al., 1995; Palombo et al., 1988; Rolland et al., 2007).

The TRN has an average firing rate of about  $20\text{--}30 \text{ s}^{-1}$  in awake cats, which correlates positively with the level of arousal and hence with the activity of the relay nuclei (Steriade et al., 1986). Raeva and Lukashev (1987) measured the activity of TRN neurons during stereotaxic surgery on subjects with dyskinesia, most of whom were parkinsonian. They found three types of cells with different discharge patterns, for which the overall mean firing rate was about  $10 \text{ s}^{-1}$ . Although information on changes in TRN activity with dopamine loss is limited, this may be taken as indirect evidence that the TRN is hypoactive in PD.

Average firing rates of the components of the BGTCS in the normal state and changes with parkinsonism are summarized in Table 1. We do not report the control rates from many of the studies in rats, because they were performed on animals under general anesthesia, which leads to significantly lower firing rates than the freely moving condition (Benazzouz et al., 2000; Kreiss et al., 1997; Pan and Walters, 1988; Rohlfs et al., 1997). Human control data are not available for most nuclei, since stereotaxic surgery is only performed in clinical cases.

### 3 Model formulation and preliminary analysis

In order to arrive at a tractable model of the dynamics governing the system in Fig. 1, we use a mean-field formulation, in which neuronal properties are spatially averaged. The dynamics are then governed by a set of equations relating the average firing rates of populations of neurons to changes in cell-body potential, which are in turn triggered by average rates of incoming pulses. This approach is based on earlier work on a model of the electrophysiology of the corticothalamic system (Rennie et al., 1999; Robinson et al., 1997, 2001a, 2003a, 2005). Section 3.1 details the basic equations of the model. Parameter values for healthy adults in the alert, eyes-open state are estimated in Sec. 3.2, and used to evaluate fixed points in Sec. 3.3. In Sec. 3.4 we review possible ways of modeling dopamine depletion.

#### 3.1 Basic equations

The first component of the model is the description of the average response of populations of neurons to changes in cell-body potential. The mean firing rate  $Q_a(V_a)$  of each population  $a$  is taken to be the maximum attainable firing rate  $Q_a^{\text{max}}$  times the proportion of neurons with a membrane potential  $V_a$  above the threshold potential  $x$ . Equivalently, the response of each neuron can be represented by a Heaviside step function  $H(V_a - x)$  multiplied by  $Q_a^{\text{max}}$ , and the population rate is given by the integral of this response times the distribution  $p(x)$  of firing thresholds,

$$Q_a(V_a) = Q_a^{\text{max}} \int_{-\infty}^{\infty} H(V_a - x)p(x)dx, \quad (1)$$

yielding the cumulative distribution function, which for a Gaussian distribution is the error function. However, the exact distribution of firing thresholds is not known, allowing us to work with

Location	Normal rate (s <sup>-1</sup> )				PD patients	MPTP-treated monkeys	6-OHDA-treated rats
	<i>Humans</i>	<i>Monkeys</i>	<i>Cats</i>	<i>Rats</i>			
Cortex		5–20 <sup>ab</sup>		2–5 <sup>c</sup>	↓ <sup>def</sup>	— <sup>a</sup>	— <sup>c</sup>
Striatum		4–7 <sup>ag</sup>		1–7 <sup>ch</sup>	↑ <sup>i</sup>	↓ <sup>g</sup> , — <sup>a</sup>	↑ <sup>klm</sup>
GPI		60–90 <sup>nopq</sup>		15–20 <sup>c</sup>	↑/— <sup>r</sup>	↑ <sup>gpst</sup> , — <sup>uv</sup>	— <sup>w</sup>
SNr		50–70 <sup>xy</sup>			— <sup>z</sup>	— <sup>w</sup>	↑ <sup>AB</sup> , ↓/— <sup>mC</sup>
GPe		40–70 <sup>noqD</sup>		35–45 <sup>E</sup>	— <sup>r</sup>	↓ <sup>qst</sup> , — <sup>a</sup>	↓ <sup>E</sup> , — <sup>m</sup>
STN		20–30 <sup>oF</sup>		8–11 <sup>G</sup>	↑ <sup>zEH</sup>	↑ <sup>u</sup>	↑ <sup>mG</sup> , — <sup>I</sup> , ↓ <sup>J</sup>
Relay nuclei	10–20 <sup>K</sup>				↓ <sup>K</sup>	↓ <sup>LMN</sup> , — <sup>O</sup>	↓ <sup>N</sup>
TRN			20–30 <sup>P</sup>		↓ <sup>Q</sup>		

Table 1: Average firing rates of the BGTCS in the healthy state, and changes with respect to this state in PD patients (compared with normal rates in monkeys, humans, or cats, as available), in MPTP-treated monkeys, and in rats treated with 6-OHDA. In the rows for GPi and GPe, changes in firing rates in rats refer to the rodent homologs of these structures, the entopeduncular nucleus (EP) and the globus pallidus (GP). Changes reflect averages; the reaction to loss of dopamine may differ in individual cases. ↑, elevated; —, no change; ↓, reduced. References: *a*, Goldberg et al. (2002); *b*, Wannier et al. (1991); *c* Dejean et al. (2008); *d*, Jenkins et al. (1992); *e* Monchi et al. (2004); *f* Monchi et al. (2007); *g*, Yoshida (1991); *h*, Kiyatkin and Rebec (1999); *i*, Magnin et al. (2000); *j* Chen et al. (2001); *k* Kish et al. (1999); *l*, Tseng et al. (2001); *m*, Walters et al. (2007); *n*, DeLong (1971); *o*, Georgopoulos et al. (1983); *p*, Kimura et al. (1996); *q*, Heimer et al. (2002); *r*, Hutchison et al. (1994); *s*, Filion and Tremblay (1991), *t*, Boraud et al. (1998); *u*, Bergman et al. (1994); *v*, Wichmann et al. (1999); *w*, Robledo and Feger (1991); *x*, DeLong et al. (1983); *y*, Schultz (1986); *z*, Hutchison et al. (1998); *A*, Benazzouz et al. (2000); *B*, Burbaud et al. (1995); *C*, MacLeod et al. (1990); *D*, DeLong et al. (1985); *E*, Pan and Walters (1988); *F*, Benazzouz et al. (2002); *G*, Kreiss et al. (1997); *H*, Levy et al. (2000); *I*, Hollerman and Grace (1992); *J*, Ni et al. (2001a); *K*, Molnar et al. (2005); *L*, Palombo et al. (1988); *M*, Gnanalingham et al. (1995); *N*, Rolland et al. (2007); *O*, Pessiglione et al. (2005); *P*, Steriade et al. (1986); *Q*, Raeva and Lukashev (1987).

the closely similar sigmoidal function

$$Q_a(\mathbf{r}, t) \equiv S_a[V_a(t)] = \frac{Q_a^{\max}}{1 + \exp[-(V_a(t) - \theta_a)/\sigma']}, \quad (2)$$

for analytical convenience. Here,  $\theta_a$  is the mean threshold potential of the population considered. Fitting (2) to the error function we find that  $\sigma'$  is  $\sqrt{3}/\pi$  times the standard deviation of the Gaussian distribution of firing thresholds (Wright and Liley, 1995). In the absence of detailed information on the standard deviations of firing thresholds in the basal ganglia, we set  $\sigma'$  equal for all populations. The function (2) increases smoothly from 0 to  $Q_a^{\max}$  as  $V_a$  runs from  $-\infty$  to  $\infty$ .

The change in the mean cell-body potential due to afferent activity depends on the mean number of synapses  $N_{ab}$  from afferent axons of type  $b$  per receiving neuron of type  $a$ , and the typical time-integrated change  $s_{ab}$  in cell-body potential per incoming pulse. Defining  $\nu_{ab} = N_{ab}s_{ab}$ , the change in the mean cell-body potential of type  $a$  neurons is thus modeled as (Robinson et al., 2004)

$$D_{\alpha\beta}(t)V_a(t) = \sum_b \nu_{ab}\phi_b(t - \tau_{ab}), \quad (3)$$

$$D_{\alpha\beta}(t) = \frac{1}{\alpha\beta} \frac{d^2}{dt^2} + \left(\frac{1}{\alpha} + \frac{1}{\beta}\right) \frac{d}{dt} + 1. \quad (4)$$

Here,  $\phi_b(t - \tau_{ab})$  is the incoming pulse rate,  $\tau_{ab}$  represents the axonal time delay for signals traveling from type  $b$  to type  $a$  neurons, and  $\alpha$  and  $\beta$  are the decay and rise rates of the cell-body potential (we assume  $\alpha < \beta$  without loss of generality). The differential operator  $D_{\alpha\beta}(t)$  is a physiologically realistic representation of dendritic and synaptic integration of incoming signals (Rennie et al., 2000; Robinson et al., 1997). The synapses and dendrites attenuate high-frequency activity due to differential delays for signals passing through them, forming an effective low-pass filter with cut-off frequency intermediate between  $\alpha$  and  $\beta$ . In general,  $\alpha$  and  $\beta$  can depend on both the sending and receiving neurons, but in order to restrict the number of parameters we take these to be equal for all populations, especially as the values of  $\alpha$  and  $\beta$  are not relevant to steady states, which are the main focus of the current paper. Future work may use different rise and decay rates for different populations, as was done for instance by Rennie et al. (2000).

In a number of previous works, neuronal activity was modeled as spreading along the cortex in a wavelike fashion (Bressloff, 2001; Bressloff et al., 2003; Jirsa and Haken, 1996, 1997; Nunez, 1995), based on consistent experimental observations of such waves of activity upon localized cortical stimulation (Burns, 1951; Chervin et al., 1988; Golomb and Amitai, 1997; Lopes da Silva and Storm van Leeuwen, 1978; Nunez, 1974; Prechtl et al., 1997; Rubino et al., 2006; Schiff et al., 2007; Wu et al., 1999; Xu et al., 2007). Estimates of characteristic axonal ranges and propagation speeds suggest that such waves are significantly damped on the scale of the human cortex (Robinson et al., 2001b, 2004; Wright and Liley, 1995). A damped-wave equation was derived in Robinson et al. (1997) using a range distribution of corticocortical fibers that decayed exponentially at large distances. Ignoring the spatial derivative, which is not relevant in the present context, this equation simplifies to

$$\frac{1}{\gamma_a^2} \left[ \frac{\partial^2}{\partial t^2} + 2\gamma_a \frac{\partial}{\partial t} + \gamma_a^2 \right] \phi_a(t) = Q_a(t), \quad (5)$$

where  $\gamma_a = v_a/r_a$  is the damping rate, consisting of the average axonal transmission speed  $v_a \simeq 5 - 10 \text{ m s}^{-1}$  and the characteristic axonal range  $r_a$ . In practice, most types of axons are short enough to justify setting  $\gamma_a = \infty$ , which has been termed the local activity approximation (Robinson et al., 2004). We therefore take only  $\gamma_e$ , the damping rate associated with cortical pyramidal cells, to yield significant propagation effects. This turns all wave equations except the cortical one into delayed one-to-one mappings. The temporal dependence in Eq. (5) is given for completeness, although we are interested in steady states.

Besides cortical excitatory cells, our model includes eight neuronal populations: cortical inhibitory ( $i$ ), striatal cells projecting to the output nuclei ( $d_1$ ), striatal cells projecting to GPe ( $d_2$ ), GPi/SNr ( $p_1$ ), GPe ( $p_2$ ), STN ( $s$ ), thalamic relay nuclei ( $s$ ), and TRN ( $r$ ). The subscript  $s$  for the relay nuclei follows the convention of earlier work, in which it referred only to specific

relay nuclei, although here we also consider the diffusely projecting CM-Pf complex. Input from the brainstem to the thalamus is denoted by a subscript  $n$ . For simplicity, we consider inhibition within the striatum of D1 to itself and D2 to itself, but not between D1 and D2.

### 3.2 Parameter values

Before proceeding to the analysis of fixed points, we here discuss how parameter values were chosen based on known physiology. Among the parameters in our model that can be relatively well measured experimentally are axonal conduction times and maximum firing rates of neuronal populations. The relative strengths of the various connections can be estimated based on experimentally determined densities of projections, types of neurotransmitters, and locations of synapses. Besides, plausible parameters should yield realistic steady-state firing rates both before and after changes that would be expected with loss of dopamine. In this section we constrain parameter values for our model using evidence from a range of studies, leading to the nominal values given in Table 2. Note that the results of the present study are independent of axonal or dendritic delays, but these values are listed for completeness and use in Paper II.

Conduction delays between neuronal populations can be estimated using antidromic or sometimes orthodromic activation, spike-triggered averaging, or cross-correlation analysis (Nowak and Bullier, 1997). The results of such studies always include axonal propagation times, but may also include dendritic and synaptic delays and neuronal integration times of the sending and/or receiving populations, depending on the method used. It is important to take this into account, since dendritic and synaptic latencies and integration times may be as long or longer than axonal propagation times (Nowak and Bullier, 1997). In addition, care is needed to determine average or characteristic delays rather than the shortest possible ones, since the former are more relevant to ongoing oscillations.

Axonal delays measured using spike timing and correlation in mice, rabbits, cats, and monkeys range from 0.1 to 5 ms for the thalamocortical projection, and 1 to 30 ms for the corticothalamic projection, with longer delays expected after scaling these values to human brain size (Roberts and Robinson, 2008). As argued in that paper, ongoing corticothalamic oscillations depend on a weighted average of conduction velocities of many fibers, further increasing the latency with respect to the values found in most experimental studies, which typically select the shortest ones. In accordance with model fits to absence seizure dynamics (Roberts and Robinson, 2008) we split the axonal propagation time for a full loop into a thalamocortical axonal delay of 35 ms and a somewhat longer corticothalamic delay of 50 ms. The hypothesis that the alpha rhythm of the EEG is caused by a resonance in a corticothalamic loop with an axonal delay of  $\sim 85$  ms has led to excellent agreement with data on a range of electrophysiological phenomena (O'Connor et al., 2002; Robinson et al., 2001a; Robinson, 2003; Breakspear et al., 2006; Kerr et al., 2008).

The corticosubthalamic pathway has been shown in some studies to act faster than transmission via the direct or indirect pathways (Bar-Gad et al., 2003). Total cortico-striato-pallidal and cortico-subthalamo-pallidal delays can be inferred from the pattern of GPe responses to cortical activation in healthy monkeys, consisting of an excitation after 8–11 ms, inhibition after 15–19 ms, and a second excitation after 26–32 ms due to disinhibition of the STN (Kita et al., 2004; Nambu et al., 2000; Yoshida et al., 1993). Since we assume synaptic and dendritic integration times of the order of 6–8 ms (time-to-peak) (Destexhe and Sejnowski, 2001; Hestrin et al., 1990), this implies that the corticosubthalamic and STN-GPe axonal delays are only about 1 ms each. The reciprocal delay from GPe to STN is also  $\lesssim 1$  ms (Nambu et al., 2000). A corticostriatal axonal delay of 2 ms and striatopallidal delay of 1 ms lead to onset of GPe excitation after about 8 ms, inhibition after 19 ms, and a second excitation after 28 ms, in accord with the above studies. The latency of postsynaptic responses in EP neurons to GP stimulation is around 3–6 ms in the rat brain slice preparation (Kita, 2001), suggesting an axonal latency of  $\lesssim 1$  ms. Anderson and Turner (1991) measured a reduction in the activity of pallidal-receiving thalamic neurons of awake monkeys generally  $< 4$  ms after stimulation of the GPi, although some cells displayed a longer latency. In anesthetized rats, the average latency of spikes in the striatum evoked by stimulation of the medial geniculate body of the thalamus was  $\sim 4$  ms (Clugnet et al., 1990). We can roughly translate this into an axonal delay of  $\sim 2$  ms in humans by noting that the value of 4 ms includes striatal integration times, but on the other hand, delays are likely to

**Table 2. Model parameters for healthy adults in the alert, eyes-open state**

Quantity	Symbol	Value	Unit	References
Corticocortical axonal range	$r_e$	80	mm	Nunez, 1995; O'Connor et al. (2002), Robinson (2003)
Cortical damping rate	$\gamma_e$	125	$s^{-1}$	Robinson et al. (2004), Rowe et al. (2004)
Synaptodendritic Decay rate	$\alpha$	160	$s^{-1}$	Destexhe and Sejnowski (2001), Hestrin et al. (1990)
Rise rate	$\beta$	640	$s^{-1}$	Destexhe and Sejnowski (2001), Hestrin et al. (1990)
Axonal delay				
$es, is$	$\tau_{es}, \tau_{is}$	35	ms	Roberts and Robinson (2008), Robinson et al. (2004), Rowe et al. (2004)
$d_1e, d_2e$	$\tau_{d_1e}, \tau_{d_2e}$	2	ms	Kimura et al. (1996), Nambu et al. (2000)
$d_1s, d_2s$	$\tau_{d_1s}, \tau_{d_2s}$	2	ms	Clugnet et al. (1990)
$p_1d_1$	$\tau_{p_1d_1}$	1	ms	Kimura et al. (1996), Nambu et al. (2000)
$p_1p_2$	$\tau_{p_1p_2}$	1	ms	Kita (2001)
$p_1\varsigma$	$\tau_{p_1\varsigma}$	1	ms	Nambu et al. (2000)
$p_2d_2$	$\tau_{p_2d_2}$	1	ms	Kimura et al. (1996), Nambu et al. (2000)
$p_2\varsigma$	$\tau_{p_2\varsigma}$	1	ms	Nambu et al. (2000)
$\varsigma e$	$\tau_{\varsigma e}$	1	ms	Bar-Gad et al. (2003), Maurice et al. (1998), Nambu et al. (2000)
$\varsigma p_2$	$\tau_{\varsigma p_2}$	1	ms	Nambu et al. (2000)
$se, re$	$\tau_{se}, \tau_{re}$	50	ms	Roberts and Robinson (2008), Robinson et al. (2004), Rowe et al. (2004)
$sp_1$	$\tau_{sp_1}$	3	ms	Anderson and Turner (1991), Uno et al. (1978)
$sr, rs$	$\tau_{sr}, \tau_{rs}$	2	ms	Voloshin and Prokopenko (1978)
Maximum firing rate				
Cortex	$Q_e^{\max}, Q_i^{\max}$	300	$s^{-1}$	McCormick et al. (1985), Steriade et al. (1998)
Striatum	$Q_{d_1}^{\max}, Q_{d_2}^{\max}$	65	$s^{-1}$	Kiyatkin and Rebec (1999)
GPe/SNr	$Q_{p_1}^{\max}$	250	$s^{-1}$	Hashimoto et al. (2003), Nakanishi et al. (1987)
GPe	$Q_{p_2}^{\max}$	300	$s^{-1}$	Cooper and Stanford (2000), Nambu and Llinás (1997a)
STN	$Q_{\varsigma}^{\max}$	500	$s^{-1}$	Kita et al. (1983), Nakanishi et al. (1987)
Relay nuclei	$Q_s^{\max}$	300	$s^{-1}$	Destexhe and Sejnowski (2003)
TRN	$Q_r^{\max}$	500	$s^{-1}$	Raeva and Lukashev (1987)
Firing threshold				
Cortex	$\theta_e, \theta_i$	14	mV	} From numerical exploration (see caption)
Striatum	$\theta_{d_1}, \theta_{d_2}$	19	mV	
GPe/SNr	$\theta_{p_1}$	10	mV	
GPe	$\theta_{p_2}$	9	mV	
STN	$\theta_{\varsigma}$	10	mV	
Relay nuclei	$\theta_s$	13	mV	
TRN	$\theta_r$	13	mV	

be slightly longer in humans than in rats (compare for instance the corticosubthalamic axonal plus dendritic and synaptic delay of  $\sim 4.5$  ms in rats, Maurice et al., 1998 with the  $\sim 6$  ms delay in monkeys, Nambu et al., 2000). Voloshin and Prokopenko (1978) measured orthodromic and antidromic response latencies of TRN neurons to stimulation of VL in cats. Interpretation of the data is complicated by the possible contribution of polysynaptic pathways, but 2 ms seems to be an adequate approximation to the monosynaptic axonal delay.

A number of studies have provided estimates of the resting membrane potentials, firing thresholds, and maximum firing rates of neurons in the basal ganglia. Most of the data come from studies of rodents, but these provide the closest possible approximation to human values, which are often not readily available. Since the biophysics determining these quantities is likely to be very similar across species, we assume that it is reasonable to use data from rodents.

The maximum firing rate of cortical regular spiking neurons is of order  $250 \text{ s}^{-1}$  (McCormick et al., 1985), whereas a class of corticothalamic fast rhythmic bursting neurons can fire up to  $\sim 400 \text{ s}^{-1}$  in either burst or tonic mode. These populations are not strictly distinct, since neocortical neurons can change their firing properties from regular spiking to fast rhythmic bursting and fast spiking depending on afferent activity (Steriade et al., 1998). The maximum rate of cortical inhibitory interneurons is of the same order as that of pyramidal neurons ( $300\text{--}600 \text{ s}^{-1}$ ), and we set  $Q_e^{\max} = Q_i^{\max} = 300 \text{ s}^{-1}$  for simplicity (cf. Sec. 3.3).

A maximum rate of  $\sim 65 \text{ s}^{-1}$  was recorded for striatal neurons in awake, freely moving rats (Kiyatkin and Rebec, 1999). High-frequency stimulation of the STN can evoke discharges up to about  $200 \text{ s}^{-1}$  in GPi cells of rhesus monkeys (Hashimoto et al., 2003), while EP neurons were found to fire at rates up to  $300 \text{ s}^{-1}$  in a rat slice preparation (Nakanishi et al., 1990). We take  $Q_{p_1}^{\max} = 250 \text{ s}^{-1}$  to be an adequate approximation. Of three types of neurons identified in the GP of guinea pigs, the most abundant type had a maximum firing rate close to  $200 \text{ s}^{-1}$  (Nambu and Llinás, 1997). On the other hand, Cooper and Stanford (2000) recorded the activity of three types of neuron in the rat GP with a weighted average maximum firing rate of  $\sim 380 \text{ s}^{-1}$ . We assume an intermediate value and let  $Q_{p_2}^{\max} = 300 \text{ s}^{-1}$ . STN neurons in rats can fire at rates up to about  $500 \text{ s}^{-1}$  (Kita et al., 1983; Nakanishi et al., 1987). Finally, low-threshold  $\text{Ca}^{2+}$  currents can cause thalamic neurons to fire high-frequency bursts at  $\sim 300 \text{ s}^{-1}$  (Destexhe and Sejnowski, 2003), while thalamic reticular neurons can fire bursts at up to  $500 \text{ s}^{-1}$  (Raeva and Lukashev, 1987).

The threshold values  $\theta_a$  are the membrane depolarizations at which the populations fire at half their maximum rate [cf. Eq. (2)]. Based on extensive exploration of physiologically realistic ranges, we choose values that give realistic steady-state firing rates for all neuronal populations in our model; these values are listed in Table 2. STN and pallidal neurons are taken to have low threshold potentials, while the threshold value is high for the relatively silent striatal neurons. Note that for  $Q \ll Q^{\max}$ , a high maximum firing rate and a low threshold  $\theta$  have closely similar effects on the (relatively low) steady-state firing rate, because

$$\frac{Q^{\max}}{1 + e^{-(V-\theta)/\sigma'}} \approx Q^{\max} e^{(V-\theta)/\sigma'}, \quad (6)$$

which means that adding  $\delta\theta$  to  $\theta$  is equivalent to replacing  $Q^{\max}$  by  $Q^{\max} e^{-\delta\theta/\sigma'}$ . Hence, it is possible that the firing thresholds and maximum firing rates are both smaller or both larger than the values used here, leaving the dynamics largely unchanged.

We also choose approximate connection strengths within physiological ranges, finding that the requirement of realistic firing rates restricts connection strengths to relatively narrow subranges. Robinson et al. (2004) derived values of  $\nu_{es}$  and  $\nu_{se}$  that satisfy both experimental constraints and give realistic firing rates in the purely corticothalamic model. Experiments in rodent neocortex in vitro (Gil et al., 1999; Thomson, 1997) and in vivo (Bruno and Sakmann, 2006) suggest that single thalamocortical and excitatory intracortical stimuli have a time-integrated response of about  $10\text{--}20 \mu\text{V s}$ . However,  $s_{es}$  should be adjusted for reduced probability of transmitter release at thalamocortical synapses upon repeated stimulation (Gil et al., 1999), and the less than additive effect of successive postsynaptic potentials (Bruno and Sakmann, 2006). If we assume the latter adjustment to yield an average unitary response of about  $12 \mu\text{V s}$ , with a release probability of 40% and  $N_{es} = 85$  (Bruno and Sakmann, 2006), we obtain  $\nu_{es} = 0.4 \text{ mV s}$ . This value is in agreement with Robinson et al. (2004), although that paper assumed a much smaller unitary response  $s_{es}$  and

a correspondingly larger number of synapses per cortical neuron. Studies of cat geniculocortical fibers suggest that the number of synapses of cortical origin per thalamic neuron far exceeds the number of thalamocortical synapses per cortical neuron (Budd, 2004; Peters and Payne, 1993). Corticothalamic fibers display paired-pulse facilitation, but often fail to evoke significant excitatory postsynaptic potentials (EPSPs) (Golshani et al., 2001; Granseth and Lindström, 2003). Unitary corticothalamic EPSPs have a small amplitude compared to retinogeniculate EPSPs, with a time-integrated response around  $12 \mu\text{V s}$  (Turner and Salt, 1998), similar to that at thalamocortical terminals. This combines with the large number of corticothalamic synapses but high failure rate to yield an approximate synaptic strength  $\nu_{se} = 0.8 \text{ mV s}$ . We assume  $\nu_{sr} = -0.4 \text{ mV s}$ , close to the value in Robinson et al. (2004). Although there are fewer inhibitory than excitatory neurons in the cortex, the synaptic strength of the inhibitory projections is larger, such that  $|\nu_{ei}| > |\nu_{ee}|$ .

Precise estimates of  $\nu_{re}$  are difficult to obtain from the literature. Although it has been estimated that  $\sim 60\%$  of TRN terminals are of cortical origin (Liu and Jones, 1999), an estimate of the total number of synapses per TRN neuron is not readily available. In mouse brain slices, the unitary postsynaptic response of TRN neurons to cortical impulses is 2–3 times greater than that of thalamic relay neurons, and the latter have a high failure rate of transmitter release ( $\sim 68\%$ ), suggesting  $s_{se} < s_{re}$ . However, paired-pulse facilitation at relay neurons may partly counterbalance this effect (Golshani et al., 2001). More importantly, the relative influences of cortical inputs to relay and TRN neurons depend on the state of alertness (Steriade et al., 1986). During drowsiness or slow-wave sleep, TRN responds to cortical stimuli with bursts of spikes, implying a relatively large  $\nu_{re}$ , while TRN neurons are tonically active during attentive wakefulness and REM sleep, implying a lower value of  $\nu_{re}$  (Steriade, 2001). This is corroborated by modeling results, which indicate that the combined influence of the cortico-reticulo-thalamic and direct corticothalamic pathways is inhibitory in sleep states, but excitatory during waking (Robinson et al., 2002). We thus model a state of alert wakefulness in which the direct corticothalamic connection is more important than the cortico-reticulo-thalamic connection, setting  $\nu_{re} = 0.15 \text{ mV s}$ .

Although a high degree of convergence of corticostriatal inputs is suggested by the large number of synaptic events per unit time in striatal neurons (Blackwell et al., 2003), the strength of corticostriatal projections is constrained by the relatively low average firing rate of striatal neurons (cf. Sec. 2.2). Corticostriatal neurons form about 5000 – 15 000 synapses per striatal cell, but each of these has a weak influence (Wilson, 1995). An immunohistochemical study found that the ipsilateral primary motor cortex innervated D1-expressing cells somewhat more strongly than D2-expressing cells (Hersch et al., 1995). We thus assume a strength per synapse of  $0.1 \mu\text{V s}$ , with 10 000 synapses per striatal D1 cell, and 7000 synapses per D2 cell, which gives  $\nu_{d_1e} = 1.0 \text{ mV s}$  and  $\nu_{d_2e} = 0.7 \text{ mV s}$ .

Steady states are very sensitive to  $\nu_{sp_1}$  due to the high firing rate of neurons in the output nuclei. In order for the thalamus not to be overly suppressed by the output nuclei we assume a relatively small connection strength  $\nu_{sp_1} = -0.03 \text{ mV s}$ . The thalamostriatal projection has been described as ‘massive’ in the squirrel monkey (Sadikot et al., 1992), but this study did not quantify its strength or extent relative to other projections. Studies in rats suggest that it is much less important than the corticostriatal projection (Groves et al., 1995). Sidibé and Smith (1996) found that intralaminar thalamic neurons preferentially innervate striatal neurons that output to GPi rather than GPe, so we let  $\nu_{d_1s} = 0.1 \text{ mV s}$  and  $\nu_{d_2s} = 0.05 \text{ mV s}$ . Evidence to suggest that  $|\nu_{p_2d_2}| > |\nu_{p_1d_1}|$  comes from a study in which anterograde transport of a tracer injected into the arm area of the primary motor cortex labeled ten times as many GPe cells as GPi cells (Strick et al., 1995). A somewhat more symmetric distribution of striatal synapses over the two pallidal segments was suggested by Shink and Smith (1995), although the innervation of GPe still appeared stronger than that of GPi. Studies on the reciprocal connections between the GPe and STN suggest that GPe exerts a powerful inhibitory control over the STN (Shink et al., 1996; Smith et al., 1990a), while the STN powerfully excites the GPe (Cheruel et al., 1996; Nambu et al., 2000; Shink et al., 1996). However, model results indicate that the GPe probably has a much weaker effect on the STN rate than vice versa, in view of stability criteria (cf. Paper II) and the comparatively high firing rate of the GPe (cf. Secs. 2.2 and 4). The STN appears to innervate both pallidal segments quite uniformly (Parent and Hazrati, 1995; Smith et al., 1990b), so we assume equal strengths for these projections. Fewer GPi synapses arise from the

GPe than from the striatum, although the GPe may exert a strong effect by forming contacts with the perikarya and proximal dendrites of GPi cells (Shink and Smith, 1995; Smith et al., 1994). Still, we assume the direct pallidopallidal projection to be weaker than other projections, since a high GPe rate would otherwise be incompatible with an even higher GPi rate (cf. Secs. 2.2 and 4). Finally, given an input  $\phi_n$ , the connection strength for projections from brainstem to thalamus,  $\nu_{sn}$ , is constrained to a relatively narrow range since large values lead to unrealistically high cortical, thalamic, and striatal rates.

### 3.3 Fixed points

Stable fixed points of the model equations, obtained assuming a constant input  $\phi_n$ , correspond to solutions at which the system settles down unless perturbed. Fixed-point equations are obtained by setting the derivatives in Eqs. (3)–(5) to zero. Denoting fixed-point values by the superscript (0), Eq. (5) yields

$$\phi_a^{(0)} = Q_a^{(0)}, \quad (7)$$

which, when substituted into Eq. (3) and using Eq. (2), gives

$$S_a^{-1} \left( \phi_a^{(0)} \right) = \sum_b \nu_{ab} \phi_b^{(0)}. \quad (8)$$

Implementing Eq. (8) for all nine neuronal populations gives a set of transcendental equations for the fixed-point firing rates  $\phi_a^{(0)}$  that can be solved numerically. These equations are simplified by imposing the *random connectivity approximation*, in which the number of synapses within the cortex is proportional to the product of the numbers of sending and receiving neurons (Braitenberg and Schüz, 1998; Robinson et al., 2001a; Wright and Liley, 1995). In the connection strengths  $\nu_{ab} = N_{ab}s_{ab}$ , the symbol  $N_{ab}$  denotes the number of synapses from neurons of type  $b$  per type  $a$  neuron, which in the random connectivity approximation thus depends only on the afferent population  $b$ . If we further assume the unitary synaptic strengths  $s_{ab}$  to be independent of the receiving population, we obtain

$$\nu_{ee} = \nu_{ie}, \quad \nu_{ei} = \nu_{ii}, \quad \nu_{es} = \nu_{is}. \quad (9)$$

For  $Q_e^{\max} = Q_i^{\max}$  and  $\theta_e = \theta_i$  (cf. Sec. 3.2) this implies, in particular, that the fixed-point values of the cortical excitatory and inhibitory firing rate fields are equal, since identical equations are obtained for  $\phi_e^{(0)}$  and  $\phi_i^{(0)}$ .

In practice, fixed points can be determined by considering the simultaneous zeros of the five functions

$$F_1(\phi_e) = \phi_e - S_e[(\nu_{ee} + \nu_{ei})\phi_e + \nu_{es}\phi_s], \quad (10)$$

$$F_2(\phi_{d_1}) = \phi_{d_1} - S_{d_1}(\nu_{d_1e}\phi_e + \nu_{d_1d_1}\phi_{d_1} + \nu_{d_1s}\phi_s), \quad (11)$$

$$F_3(\phi_{d_2}) = \phi_{d_2} - S_{d_2}(\nu_{d_2e}\phi_e + \nu_{d_2d_2}\phi_{d_2} + \nu_{d_2s}\phi_s), \quad (12)$$

$$F_4(\phi_{p_2}) = \phi_{p_2} - S_{p_2}[\nu_{p_2d_2}\phi_{d_2} + \nu_{p_2p_2}\phi_{p_2} + \nu_{p_2s}S_\zeta(\nu_{\zeta e}\phi_e + \nu_{\zeta p_2}\phi_{p_2})], \quad (13)$$

$$F_5(\phi_s) = \phi_s - S_s(\nu_{se}\phi_e + \nu_{sp_1}\phi_{p_1} + \nu_{sr}\phi_r + \nu_{sn}\phi_n). \quad (14)$$

First an initial estimate of the thalamic firing rate  $\phi_s$  is made. For the given choice of  $\phi_s$ , the cortical excitatory rate  $\phi_e$  is uniquely determined by the zero of  $F_1$ , as shown in Fig. 2(a) using the parameter values in Table 2. From this the striatal rates  $\phi_{d_1}$  and  $\phi_{d_2}$  can be determined using the functions  $F_2$  and  $F_3$ . These are negative at  $\phi_{d_1}, \phi_{d_2} = 0$  and positive at the maximum striatal firing rates, crossing zero exactly once since  $\nu_{d_1d_1} < 0$  and  $\nu_{d_2d_2} < 0$  ensure that their derivatives

$$\frac{dF_2(\phi_{d_1})}{d\phi_{d_1}} = 1 - \nu_{d_1d_1} Q_{d_1}^{\max} \frac{\exp[-(\nu_{d_1e}\phi_e + \nu_{d_1d_1}\phi_{d_1} + \nu_{d_1s}\phi_s - \theta_{d_1})/\sigma']}{\sigma' \{1 + \exp[-(\nu_{d_1e}\phi_e + \nu_{d_1d_1}\phi_{d_1} + \nu_{d_1s}\phi_s - \theta_{d_1})/\sigma']\}^2}, \quad (15)$$

$$\frac{dF_3(\phi_{d_2})}{d\phi_{d_2}} = 1 - \nu_{d_2d_2} Q_{d_2}^{\max} \frac{\exp[-(\nu_{d_2e}\phi_e + \nu_{d_2d_2}\phi_{d_2} + \nu_{d_2s}\phi_s - \theta_{d_2})/\sigma']}{\sigma' \{1 + \exp[-(\nu_{d_2e}\phi_e + \nu_{d_2d_2}\phi_{d_2} + \nu_{d_2s}\phi_s - \theta_{d_2})/\sigma']\}^2}, \quad (16)$$

are always positive. The functions  $F_2$  and  $F_3$  are shown in Figs. 2(b) and 2(c). The striatal rates increase with both the thalamic rate  $\phi_s$  and the cortical rate  $\phi_e$ . The unique zero of the function

$F_4$  determines the GPe rate  $\phi_{p_2}$ . The value of  $\phi_{p_2}$  first decreases, then increases slightly with both  $\phi_s$  and  $\phi_e$  [Fig. 2(d)]. Knowing  $\phi_{p_2}$  in turn allows determination of the STN and GPi/SNr rates  $\phi_s$  and  $\phi_{p_1}$ , and finally, the self-consistency relation  $F_5 = 0$  must be satisfied for  $\phi_s$  to represent a fixed point. The value of  $F_5$  is negative at  $\phi_s = 0$ , and positive at  $\phi_s = Q_s^{\max}$ , since the last term in (14) is always smaller than  $Q_s^{\max}$ . By continuity of  $F_5$ , there is always at least one fixed point, and in general an odd number of fixed points. The function  $F_5$  plotted in Fig. 2(e) shows that there are three fixed points for the parameters in Table 2. Since the low-firing-rate fixed point for  $\phi_s$  is stable and yields the most realistic firing rates for all populations, we will take this fixed point to represent the physiological situation. It is important to note that we obtain realistic steady states with parameter values that are consistent with experimental findings (cf. Sec. 3.2); this is a fundamental test of the physiological realism of the model. Figs. 2(e) and 2(f) show that all firing rates increase with the brainstem input  $\phi_n$ .

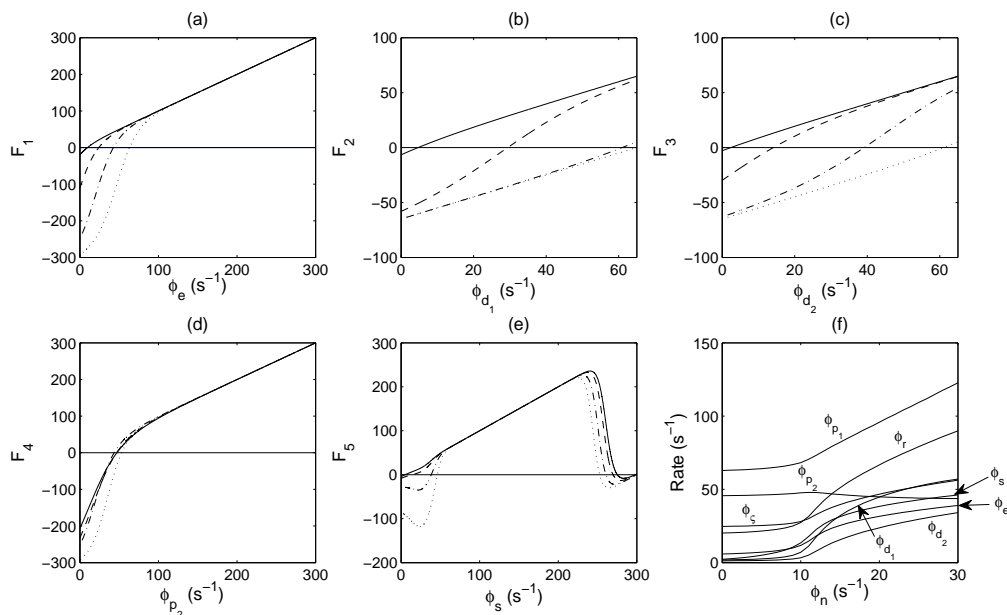


Figure 2: Equilibrium firing rates of the BGTCS. (a)–(d) Equilibrium values of  $\phi_e$ ,  $\phi_{d_1}$ ,  $\phi_{d_2}$ , and  $\phi_{p_2}$  (zeros of  $F_1 - F_4$ ) for different thalamic rates  $\phi_s$ . Solid,  $\phi_s = 10 \text{ s}^{-1}$ ; dashed,  $\phi_s = 30 \text{ s}^{-1}$ ; dash-dotted,  $\phi_s = 50 \text{ s}^{-1}$ ; dotted,  $\phi_s = 70 \text{ s}^{-1}$ . (e) Equilibrium values of  $\phi_s$  (zeros of  $F_5$ ) for different external inputs  $\phi_n$ . Solid,  $\phi_n = 5 \text{ s}^{-1}$ ; dashed,  $\phi_n = 10 \text{ s}^{-1}$ ; dash-dotted,  $\phi_n = 20 \text{ s}^{-1}$ ; dotted,  $\phi_n = 30 \text{ s}^{-1}$ . (f) Dependence of low-firing-rate fixed points on  $\phi_n$ .

### 3.4 Modeling dopamine depletion

It is widely recognized that dopamine modulates corticostriatal transmission both presynaptically and postsynaptically (Calabresi et al., 2000). However, observations on these effects are complicated and sometimes paradoxical. For instance, dopamine may facilitate glutamate-induced activity at low concentrations, but be inhibitory at higher concentrations (Hu and White, 1997). Joint activation of D1 and D2 receptors may have a supra-additive effect on striatal neurons, and upregulation of both receptor types after dopamine depletion may influence corticostriatal transmission (Hu et al., 1990).

Nevertheless, some findings are relatively consistent across studies. Dopamine appears to have a predominantly inhibitory effect via D1 receptors when striatal neurons are in a hyperpolarized state (Nicola and Malenka, 1998), but a facilitatory effect when they are already in an activated state (Hernández-López et al., 1997; Nicola et al., 2000). Such facilitation via D1 activation may primarily affect NMDA receptor-mediated transmission (Cepeda et al., 1998; Levine et al., 1996). In line with these observations, some researchers have suggested that dopamine increases

the signal-to-noise ratio (SNR) in the striatum, making medium spiny neurons sensitive only to strong inputs (Nicola et al., 2004; O'Donnell, 2003). This is supported by the finding that dopamine reduces the basal level of striatal activity, but enhances the phasic response to glutamate (Kiyatkin and Rebec, 1996). To model the reduction in SNR following loss of dopamine, Leblois et al. (2006) suggested decreasing the firing thresholds of striatal neurons as well as corticostriatal connection strengths to both D1- and D2-expressing neurons. They assumed both thresholds and connection strengths to depend nearly linearly on the level of dopamine. We use

$$\theta_{d_1}^{\text{new}} = \theta_{d_1} - h\chi; \quad \theta_{d_2}^{\text{new}} = \theta_{d_2} - h\chi, \quad (17)$$

$$\nu_{d_1e}^{\text{new}} = \nu_{d_1e} - \chi; \quad \nu_{d_2e}^{\text{new}} = \nu_{d_2e} - \chi, \quad (18)$$

where we consider  $h = 5, 10, \text{ and } 15 \text{ s}^{-1}$ , and  $\chi$  between 0 and 0.6 mV s. Note that the effective thresholds of D1 and D2 neurons are approximated as equal for simplicity, although their intrinsic properties may differ in practice (Moyer et al., 2007).

In contrast to the above possibility, dopamine loss may also reduce transmission via D1-expressing cells and enhance transmission via D2-expressing cells. In support of this possibility, a number of studies have shown that depression of excitation via glutamatergic, particularly AMPA, receptors follows activation of D2 receptors (Hsu et al., 1995; Levine et al., 1996; Toan and Schultz, 1985; Umemiya and Raymond, 1997). Furthermore, Mallet et al. (2006) found an increase in both the spontaneous activity and responsiveness of striatopallidal neurons after dopamine depletion, whereas striatonigral neurons became less active. Mallet and coworkers suggested that this imbalance may be exacerbated by feedforward inhibition by fast-spiking GABAergic interneurons, which narrow the time window for integration of cortical inputs in striatonigral neurons, and widen the time window in striatopallidal neurons, leading to inappropriate summation of signals in the indirect pathway. This possibility can be modeled by simultaneously increasing the strength of corticostriatal projections giving rise to the indirect pathway, and decreasing that of projections giving rise to the direct pathway. In the absence of detailed information concerning the relative sizes of the changes in these connection strengths, we decrease  $\nu_{d_1e}$  and increase  $\nu_{d_2e}$  by the same factor  $\xi$ . We also consider the effects of modulating  $\nu_{d_1e}$  and  $\nu_{d_2e}$  independently. Of course, the degree of differential modulation of the direct and indirect pathways by dopamine depletion is limited by the extent of segregation of D1 and D2 class receptors, and the separation of striatal projections to GPI/SNr and GPe. Nevertheless, differential modulation may occur with only a partial distinction between the direct and indirect pathways.

Reduced release of dynorphin and enhanced release of enkephalin in the striatum are thought to represent compensatory mechanisms that oppose the effects of chronic dopamine depletion (Augood et al., 1989; Betarbet and Greenamyre, 2004; Engber et al., 1992). For instance, dynorphin appears to inhibit the release of dopamine in the striatum, and oppose the effects of D1-receptor stimulation on striatonigral neurons (Steiner and Gerfen, 1998). Therefore, the loss of dynorphin will enhance the sensitivity of D1-expressing neurons to the remaining dopamine. Dynorphin and enkephalin may also affect striatal input to the GPe as well as intrapallidal inhibition (Ogura and Kita, 2000; Stanford and Cooper, 1999). Enkephalin appears to act presynaptically via opioid receptors to inhibit the release of GABA at both striatopallidal and intrapallidal terminals (Maneuf et al., 1994; Stanford and Cooper, 1999), decreasing the corresponding connection strengths. These effects may be partly opposed by loss of dynorphin from axon collaterals of neurons projecting to both pallidal segments (Ogura and Kita, 2000). Furthermore, the loss of direct dopaminergic afferentation promotes GABA release at striato-GPe terminals through the action of presynaptic D2 receptors (Floran et al., 1997; Querejeta et al., 2001). Assuming that striatopallidal transmission is more affected by dopamine loss than by enkephalin, we model PD with an increase in striato-GPe inhibition. The prevalence of enkephalin over dynorphin in the GPe suggests that the strength of intrapallidal inhibition is reduced. This agrees with the suggestion of Terman et al. (2002) that dopaminergic denervation weakens the lateral connections in the GPe, although they assumed enkephalin and dynorphin to exert concerted rather than opposing effects. Reduced dynorphin levels may also depolarize GPe neurons by blocking membrane potassium conductance (Ogura and Kita, 2000), which we model by lowering the corresponding threshold potential.

Several lines of evidence indicate that STN overactivity is not only caused by reduced GPe firing. For instance, GPe lesions only cause a slight increase in STN rate (Hassani et al., 1996),

and blockade of glutamatergic transmission suppresses STN overactivity in rats with haloperidol-induced akinesia (Miwa et al., 1998). Increased enkephalin levels may inhibit GABAergic synaptic transmission via  $\mu$ -opioid receptors, which are expressed in high concentration in the human STN (Peckys and Landwehrmeyer, 1999; Raynor et al., 1995), although enkephalin also suppresses excitatory transmission (Shen and Johnson, 2002). Studies in rats have suggested that enhanced excitation by the thalamic parafascicular nucleus (Orioux et al., 2000) and/or the pedunculopontine nucleus (PPN) (Breit et al., 2001, 2006; Orioux et al., 2000) may contribute to STN hyperactivity in parkinsonism. Rats treated with 6-OHDA have elevated levels of extracellular potassium in the STN, possibly due to changes in conductivity and delayed clearance, which increases the activity of this nucleus (Strauss et al., 2008). Furthermore, the extracellular concentration of glutamate is increased (Fujikawa et al., 1996), and that of GABA decreased (Engblom et al., 2003), by higher extracellular levels of potassium. We model the hyperexcitability of STN neurons in PD by reducing their average threshold potential.

The frontal lobe, including the prefrontal cortex, SMA, and M1, receives a significant dopaminergic innervation from the SNc, VTA, and retrorubral area (Gaspar et al., 1992; Williams and Goldman-Rakic, 1993). The predominant influence of dopamine on prefrontal pyramidal cell firing is inhibitory, due to enhanced synaptic inputs from GABAergic interneurons (Gulledge and Jaffe, 2001; Sesack and Bunney, 1989; Zhou and Hablitz, 1999). Gulledge and Jaffe (2001) suggested that this is because of enhanced GABA release by interneurons independent of their spike rate, implying increased synaptic strengths  $|\nu_{ei}|$  and  $|\nu_{ii}|$ . Dopamine also renders interneurons more susceptible to excitatory inputs from pyramidal cells, apparently without affecting their firing threshold or the amplitude of EPSPs (Gao and Goldman-Rakic, 2003). This mechanism has no precise equivalent in our model, but can be approximated by an increased synaptic strength  $\nu_{ie}$ . Furthermore, changes in intrinsic currents increase the excitability of pyramidal neurons of the rat prefrontal cortex after D1 receptor activation in vitro (Thurley et al., 2008), which may positively affect  $\nu_{ee}$ . This suggests that we can model PD in part by decreasing the synaptic strengths  $\nu_{ee}$ ,  $\nu_{ie}$ , and especially  $|\nu_{ei}|$  and  $|\nu_{ii}|$ , in accord with the reduced intracortical inhibition observed upon transcranial magnetic stimulation in PD patients off medication (Ridding et al., 1995).

We thus model the effects of nigrostriatal degeneration in the following five ways:

- (I) mimicking a decrease in striatal SNR by reducing both firing thresholds and corticostriatal connection strengths according to Eqs. (17) and (18);
- (II) increasing  $\nu_{d_2e}$  and decreasing  $\nu_{d_1e}$  either individually or by the same factor  $\xi$ , in agreement with the direct/indirect pathway model;
- (III) reducing lateral inhibition in the GPe, which mimicks enhanced levels of enkephalin;
- (IV) attenuating cortical interactions to capture loss of intrinsic cortical dopamine;
- (V) a combination of a stronger indirect and weaker direct pathway ( $\nu_{d_1e} = 0.5$  mV s,  $\nu_{d_2e} = 1.4$  mV s), reduced intrapallidal inhibition ( $\nu_{p_2p_2} = -0.07$  mV s), weaker intracortical coupling ( $\nu_{ee} = \nu_{ie} = 1.4$  mV s,  $\nu_{ei} = \nu_{ii} = -1.6$  mV s), lower STN and GPe firing thresholds ( $\theta_{p_2} = 8$  mV,  $\theta_{\zeta} = 9$  mV), and a stronger striato-GPe projection ( $\nu_{p_2d_2} = -0.5$  mV s). We will call the state corresponding to these parameters the ‘full parkinsonian state’.

## 4 Results

We now describe the results of applying the model equations to the system of connections depicted in Fig. 1. The steady-state firing rates corresponding to the parameter values in Table 2, with a stimulus level of  $10 \text{ s}^{-1}$ , are listed in column *a* of Table 3. All rates are in physiologically realistic ranges for healthy individuals if the average striatal rate is taken to be  $(\phi_{d_1} + \phi_{d_2})/2$  (cf. Table 1). Changes in firing rates are derived when modeling dopamine loss in the five ways listed in Sec. 3.4. Model predictions are compared with the empirical findings summarized in Sec. 2.2.

### *Effects of parameter changes mimicking a reduced signal-to-noise ratio*

Irrespective of the relative sizes of the changes in striatal firing thresholds and corticostriatal connection strengths, a reduction in SNR simulated by increasing  $\chi$  [cf. Eqs. (17) and (18)] has little impact on average firing rates (cf. Fig. 3). Representative rates are listed for  $h = 10 \text{ s}^{-1}$

	<i>a</i>	<i>b</i>	<i>c</i>	<i>d</i>	<i>e</i>	<i>f</i>	<i>g</i>	<i>h</i>	<i>i</i>	<i>j</i>	<i>k</i>	<i>l</i>	<i>m</i>	<i>n</i>	<i>o</i>
Cortex	12	12	10	16	12	22	14	12	13	12	13	11	10	14	10
D1	7.4	6.0	1.9	14	2.4	24	2.8	2.2	15	2.6	13	6.7	5.0	11	5.1
D2	3.5	2.7	9.3	6.4	12	11	16	12	5.4	24	3.9	5.8	2.5	4.9	2.6
GPi/SNr	69	69	83	49	70	78	100	110	63	110	64	72	87	56	85
GPe	48	48	40	65	51	48	36	47	46	28	48	45	47	58	55
STN	28	28	29	27	27	36	33	36	29	34	29	29	27	27	32
Relay nuclei	14	14	11	20	13	22	13	10	15	10	15	13	10	17	11
TRN	28	28	25	34	27	42	29	27	29	27	29	27	25	31	25

Table 2: Firing rates of the components of the BGTCS (in  $s^{-1}$ ) corresponding to the following cases: (a) healthy state, as represented by the parameters in Table 2; (b) reduced-SNR state, obtained from *a* by setting  $h = 10 s^{-1}$ ,  $\chi = 0.6 mV s$ , which leads to  $\theta_{d_1} = \theta_{d_2} = 13 mV$ ,  $\nu_{d_1e} = 0.4 mV s$ ,  $\nu_{d_2e} = 0.1 mV s$ ; (c) state *a* with a stronger indirect and weaker direct pathway,  $\nu_{d_1e} = 0.5 mV s$  and  $\nu_{d_2e} = 1.4 mV s$ ; (d) state *a* with weaker intrapallidal inhibition  $\nu_{p_2p_2} = -0.03 mV s$ ; (e) state *c* with  $\nu_{p_2p_2} = -0.03 mV s$ ; (f) state *a* with weaker cortical interactions,  $\nu_{ee} = \nu_{ie} = 1.4 mV s$ ,  $\nu_{ei} = \nu_{ii} = -1.6 mV s$ ; (g) state *c* with  $\nu_{ee} = \nu_{ie} = 1.4 mV s$ ,  $\nu_{ei} = \nu_{ii} = -1.6 mV s$ ; (h) full parkinsonian state' (cf. Sec. 3.4); (i) state *a* with  $\nu_{d_1d_1} = \nu_{d_2d_2} = 0 mV s$ ; (j) state *g* with  $\nu_{d_1d_1} = \nu_{d_2d_2} = 0 mV s$ ; (k) state *a* with  $\nu_{d_1s} = 0.3 mV s$ ; (l) state *a* with  $\nu_{d_2s} = 0.3 mV s$ ; (m) state *a* with  $\nu_{p_1p_2} = 0 mV s$ ; (n) state *a* with  $\nu_{p_2s} = 0.4 mV s$ ; (o) state *a* with  $\nu_{s_e} = 0.2 mV s$ . Input to the thalamic relay nuclei is  $10 s^{-1}$  and all rates are given to two significant figures.

and  $\chi = 0.6 mV s$  in Column *b* of Table 3. In the model of Leblois et al. (2006), which lacks an indirect pathway but in which dopamine loss is also modeled by approximating a reduced SNR, resting activity in the GPi also changes little with a lower dopamine level, whereas cortical activity shows a small increase. The model of Leblois et al. (2006) is not directly comparable to ours, since it contains a different set of connections, forming separate streams in the direct path but with diffuse projections from STN to GPi in the hyperdirect pathway. Furthermore, it considers individual neurons with linear response functions above threshold, a different form of the dendritic/synaptic filter function, and identical firing thresholds for different neurons in each given population except the striatal one, whereas the sigmoid function (2) results from a distribution of firing thresholds. However, their (deliberately) small change in average activity with a reduced SNR corresponds well with our result.

#### *Effects of stronger indirect and weaker direct pathway*

A simultaneous increase in  $\nu_{d_2e}$  and decrease in  $\nu_{d_1e}$  by an identical factor  $\xi$  leads to changes in firing rates that agree well with the average of a cross-section of empirical findings [cf. Fig. 4(a) and Table 1]: GPe and thalamic rates are reduced, while STN and GPi/SNr rates are elevated. Because the increase in D2 rate is greater than the reduction in D1 rate, the overall striatal rate is slightly increased. Figure 4(b) and 4(c) show that these changes are effected mainly through the indirect pathway, since a weaker  $\nu_{d_1e}$  decreases  $\phi_s$ ,  $\phi_{d_1}$ , and  $\phi_{d_2}$ , and barely affects  $\phi_{p_2}$ . Doubling the strength of the indirect pathway while reducing that of the direct pathway by the same factor ( $\nu_{d_1e} = 0.5 mV s$  and  $\nu_{d_2e} = 1.4 mV s$ ) leads to the rates in Column *c* of Table 3.

The sizes of these changes are fairly realistic, with a relatively large change in the rate of the output nuclei and smaller changes in cortical, thalamic, and average (over the D1 and D2 populations) striatal rates (cf. Sec. 2.2), but the increase in STN activity is smaller than would be expected on the basis of empirical evidence, while the decrease in GPe activity is quite large. Although our model predicts that GPe lesion increases the rate of the remaining intact GPe neurons (cf. Paper II), lesions are nevertheless expected to decrease the total GPe output. Therefore, our finding that a relatively large decrease in GPe output only slightly enhances STN firing accords with the results of GPe lesion reported by Hassani et al. (1996), and confirms the influence of other excitatory mechanisms on the STN rate mentioned in Sec. 3.4.

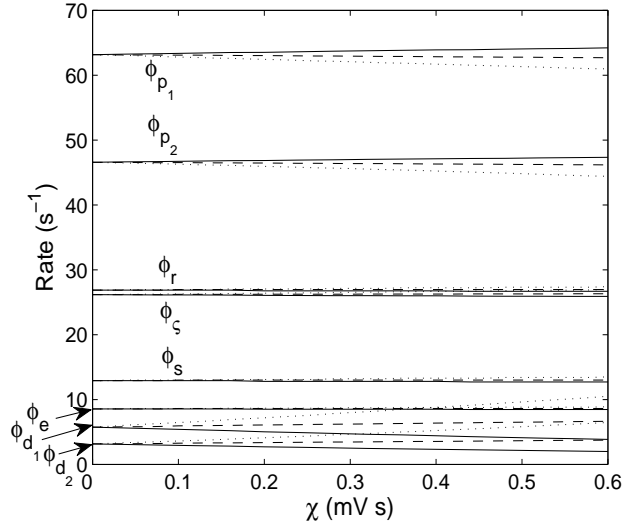


Figure 3: Changes in firing rates due to reduction in striatal SNR. The parameter  $h$  in Eq. (17) is taken to be either  $5 \text{ s}^{-1}$  (solid),  $10 \text{ s}^{-1}$  (dashed), or  $15 \text{ s}^{-1}$  (dotted). Groups of lines start together at  $\chi = 0 \text{ mV s}$ .

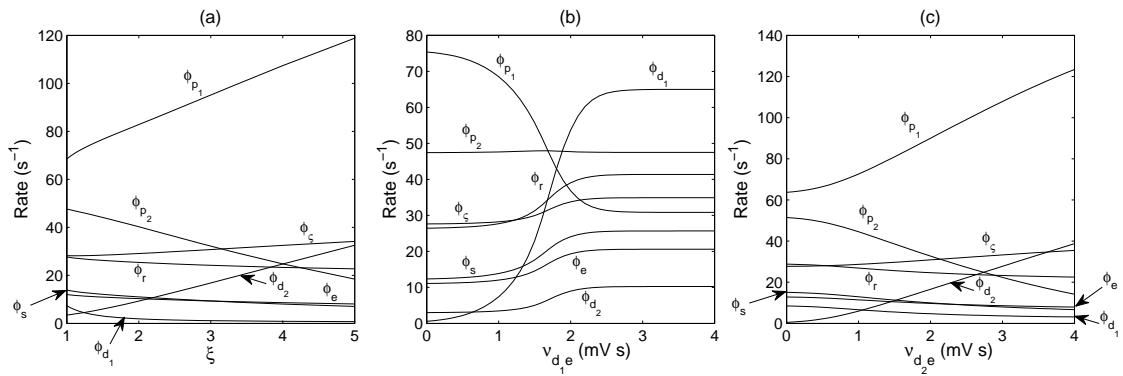


Figure 4: Changes in firing rates when modeling dopamine loss by an increase in  $\nu_{d2e}$  and decrease in  $\nu_{d1e}$ . (a) Rates when multiplying  $\nu_{d2e}$  and dividing  $\nu_{d1e}$  by the same factor  $\xi$ . (b) Rates vs.  $\nu_{d1e}$ . (c) Rates vs.  $\nu_{d2e}$ .

### Effects of weakened intrapallidal inhibition

Figure 5(a) shows the results of weakened lateral inhibition in the GPe. The effects on the pallidal and STN rates are opposite to those expected in PD, in line with the presumed compensatory effects of increased enkephalin levels with chronic dopamine depletion. Figures 5(b)–(d) illustrate how a combination of weakened intrapallidal inhibition and a reduced SNR [ $h = 10 \text{ s}^{-1}$  in Eq. (17)] affects the GPi/SNr, GPe, and STN rates, respectively. The corresponding results for a weakened direct and strengthened indirect pathway are shown in Figs. 5(e)–(g). The reduction in  $|\nu_{p_2p_2}|$  causes parkinsonian rates to be reached more slowly with an increase in  $\xi$ . Column  $d$  of Table 3 contains the steady-state firing rates for  $\nu_{p_2p_2} = -0.03 \text{ mV s}$ , where  $\chi = 0 \text{ mV s}$  and  $\xi = 1$ . The rates for  $\nu_{d_1e} = 0.5 \text{ mV s}$ ,  $\nu_{d_2e} = 1.4 \text{ mV s}$ , and  $\nu_{p_2p_2} = -0.03 \text{ mV s}$  are given in Column  $e$ .

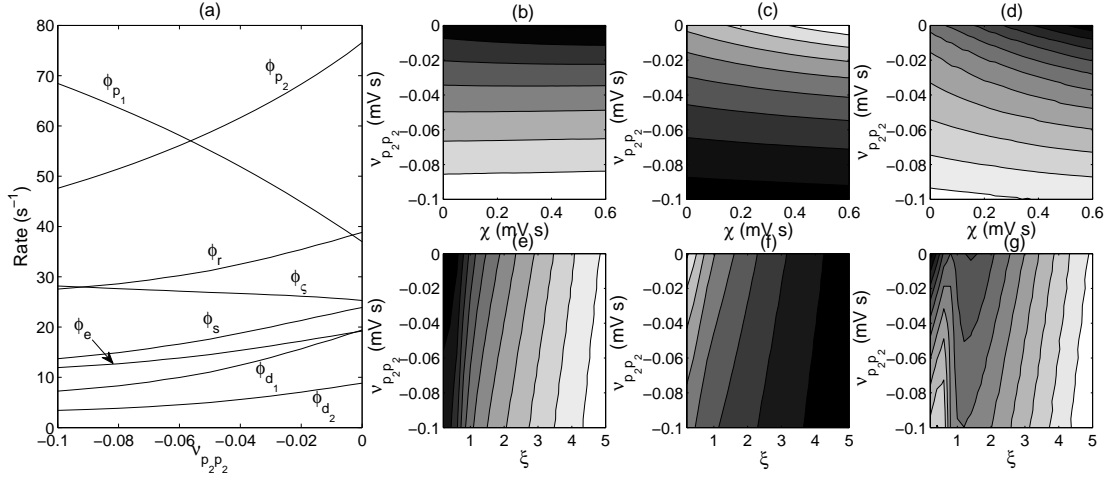


Figure 5: Sensitivity of steady-state firing rates to lateral inhibition in the GPe. (a) Changes in pallidal and STN rates with smaller  $|\nu_{p_2p_2}|$  are opposite to those in parkinsonism. (b)–(d) From left to right: contour plots of GPi/SNr, GPe, and STN rates as functions of  $\nu_{p_2p_2}$  and striatal SNR, where  $h = 10 \text{ s}^{-1}$  [cf. Eqs. (17) and (18)]. (e)–(g) From left to right: contour plots of GPi/SNr, GPe, and STN rates as functions of  $\nu_{p_2p_2}$  and the relative strengths of the direct and indirect pathways. Lighter shades correspond to higher rates.

### Effects of weakened cortical interactions

Loss of intrinsic cortical dopamine due to degeneration of the mesocortical pathway is expected to reduce intracortical coupling, and especially the strength of inhibition. Due to the random connectivity approximation (cf. Sec. 3.3), steady-state firing rates depend only on the sum  $\nu_{ee} + \nu_{ei}$ , rather than on the individual connection strengths. The sensitivity of the firing rates of the various components to this sum is depicted in Fig. 6. It is seen that loss of mesocortical dopamine helps to normalize the cortical rate after nigrostriatal damage, and further increases the STN rate. The effect on the GPe rate depends on the relative strengths of the direct and indirect pathways: it remains almost constant with mesocortical dopamine loss if the SNc is intact, but decreases with mesocortical dopamine loss after SNc lesion (modeled with  $\nu_{d_1e} = 0.5 \text{ mV s}$  and  $\nu_{d_2e} = 1.4 \text{ mV s}$ ). The rates for  $\nu_{ee} = \nu_{ie} = 1.4 \text{ mV s}$  and  $\nu_{ei} = \nu_{ii} = -1.6 \text{ mV s}$  are listed in Column  $f$  of Table 3, with the corresponding values where also  $\nu_{d_1e} = 0.5 \text{ mV s}$  and  $\nu_{d_2e} = 1.4 \text{ mV s}$  in Column  $g$ .

### Effects of GPe and STN firing thresholds and the striato-GPe projection

Besides the above changes, nigrostriatal degeneration may lead to reduced STN and GPe firing thresholds and an increase in  $|\nu_{p_2d_2}|$ , as discussed in Sec. 3.4. Changes in firing rates with  $\theta_{p_2}$  and  $\theta_c$  are shown in Fig. 7, where nigrostriatal and mesocortical dopamine loss are taken into

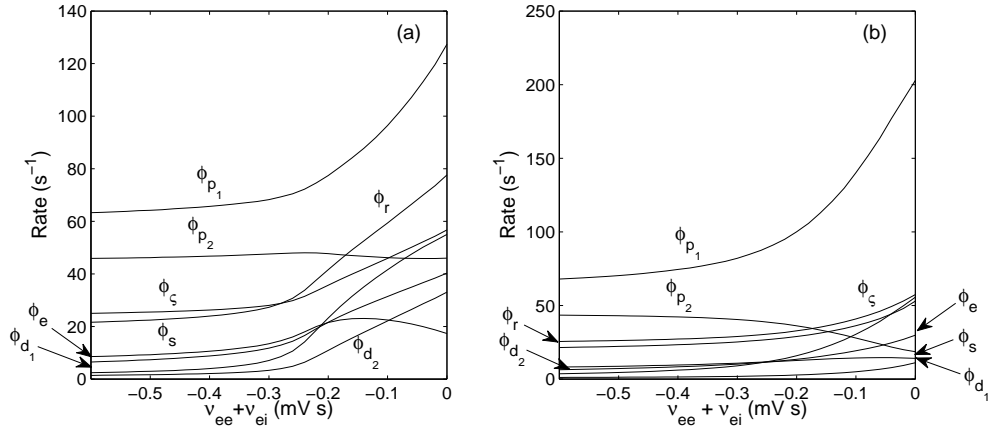


Figure 6: Sensitivity of steady-state firing rates to intracortical connection strengths. Rates only depend on the sum  $\nu_{ee} + \nu_{ei}$  due to the random connectivity approximation (cf. Sec. 3.3). (a) Variations with respect to the healthy state. (b) Variations with respect to the state with  $\nu_{d_1e} = 0.5$  mV s,  $\nu_{d_2e} = 1.4$  mV s.

account via  $\nu_{d_1e} = 0.5$  mV s,  $\nu_{d_2e} = 1.4$  mV s,  $\nu_{ee} = \nu_{ie} = 1.4$  mV s, and  $\nu_{ei} = \nu_{ii} = -1.6$  mV s. A reduction in  $\theta_{p_2}$  normalizes all rates that were altered by SNc lesion, except that of striatal D2 cells. A smaller  $\theta_\zeta$  has the opposite effect apart from increasing the GPe rate. Together, lower STN and GPe firing thresholds limit the decrease in GPe rate, counterbalance the increase in corticothalamic and striatal rates caused by mesocortical dopamine loss, and help account for a relatively large increase in STN rate.

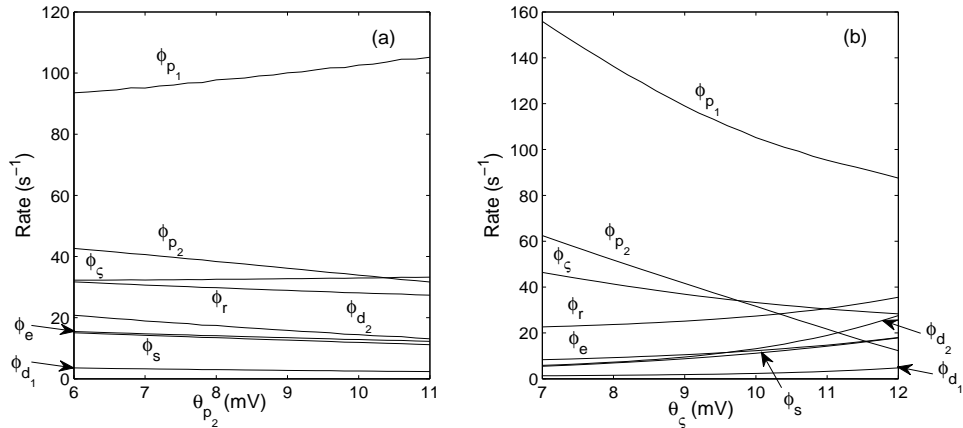


Figure 7: Sensitivity of steady-state firing rates to STN and GPe firing thresholds, where  $\nu_{d_1e} = 0.5$  mV s,  $\nu_{d_2e} = 1.4$  mV s,  $\nu_{ee} = \nu_{ie} = 1.4$  mV s, and  $\nu_{ei} = \nu_{ii} = -1.6$  mV s to mimic nigrostriatal and mesocortical dopamine depletion. (a) Dependence on  $\theta_{p_2}$ . (b) Dependence on  $\theta_\zeta$ .

Figure 8 shows the sensitivity of the steady-state firing rates to the remaining connection strengths, with all other parameters held constant at the values in Table 2. The shaded regions indicate parameter ranges that yield realistic discharge rates in the healthy state for all neuronal populations (cf. Sec. 2.2). It is seen that a stronger striato-GPe projection causes larger increases in STN and GPi/SNr rates, and a larger decrease in GPe rate. The change in GPe rate therefore depends on the relative changes in  $\nu_{p_2d_2}$ ,  $\nu_{d_1e}$ ,  $\nu_{d_2e}$ ,  $\nu_{ee}$ , and  $\nu_{ei}$  on the one hand, and  $\theta_{p_2}$  and  $\theta_\zeta$  on the other, in agreement with the range of experimental findings (Boraud et al., 1998; Fillion and Tremblay, 1991; Goldberg et al., 2002; Heimer et al., 2002;

Hutchison et al., 1994; Magill et al., 2001; Pan and Walters, 1988; Walters et al., 2007). Equilibrium rates for the full parkinsonian state are given in Column  $h$  of Table 3.

### *Effects of remaining projections*

We now consider the effects of the various projections that are not included in the classic direct/indirect pathway model. Firing rates are not highly sensitive to local striatal inhibition (cf. Fig. 8). Removing it altogether ( $\nu_{d_1 d_1} = \nu_{d_2 d_2} = 0$  mV s) slightly increases all rates except those of the GPe and output nuclei, which are decreased (Table 3 Column  $i$ ). The steady-state solutions for  $\nu_{d_1 d_1} = \nu_{d_2 d_2} = 0$  mV s in the full parkinsonian state are given in Column  $j$  of Table 3. Comparison of the difference between Columns  $a$  and  $h$ , and that between Columns  $i$  and  $j$ , reveals that larger  $|\nu_{d_1 d_1}|$  and  $|\nu_{d_2 d_2}|$  help to attenuate alterations in all rates due to dopamine depletion. Increasing  $\nu_{d_1 s}$  to 0.3 mV s predictably leads to a higher D1 rate, also increasing all other rates except that of the GPi/SNr (Column  $k$ ). Increasing the strength of the thalamo-D2 projection to  $\nu_{d_2 s} = 0.3$  mV s reduces the GPe rate, which in turn leads to a slightly higher STN rate, elevated GPi/SNr activity, and suppression of corticothalamic targets (Column  $l$ ). To assess the influence of the GPe-GPi/SNr projection we let  $\nu_{p_1 p_2} = 0$  mV s. This reduces all rates except that of the output nuclei (Column  $m$ ). A stronger STN-GPe projection ( $\nu_{p_2 s} = 0.4$  mV s) greatly increases the GPe rate, leading to a reduction in the activity of the output nuclei, which increases corticothalamic and striatal rates (Column  $n$ ). By providing a stronger drive to the STN, a larger  $\nu_{s e}$  increases the rates of both STN and its target nuclei. As a result, thalamic activity is suppressed, reducing both cortical and striatal rates. Column  $o$  of Table 3 lists the rates for  $\nu_{s e} = 0.2$  mV s.

## 5 Summary and Discussion

We have formulated a mean-field model of the basal ganglia-thalamocortical system (BGTCS) that yields realistic steady-state firing rates with parameters in physiologically plausible ranges, and takes into account many projections that were excluded from previous models. Estimates of parameter values and firing rates in health and in Parkinson’s disease (PD) were based on an extensive review of the experimental literature. After deriving expressions for the steady states, we have explored the effects of dopamine loss on the average firing rates of the basal ganglia nuclei, thalamus, and cortex. The influence of a range of connection strengths on these changes in firing rates was assessed. The model provides a framework for studying the electrophysiology of the interconnected basal ganglia, thalamus, and cortex, based on previous work by Rennie et al. (1999); Robinson et al. (1997, 2001a, 2003a, 2005). Furthermore, it lays the foundation for analysis of dynamics and oscillations in PD, considered in Paper II (Van Albada et al., 2009). Our main results are the following:

(i) A decrease in the strength of cortical projections to striatal D1 neurons and a simultaneous increase in that to striatal D2 neurons, as in the direct/indirect pathway model (Albin et al., 1989; Alexander and Crutcher, 1990), causes elevated GPi/SNr and STN rates and reduced GPe and thalamic rates, in agreement with the findings of many experimental studies of animal models of PD. However, a stronger indirect pathway alone, without modulation of the direct pathway, may be sufficient to approximate empirical results. Therefore, our results are not predicated on a complete separation between the direct and indirect pathways. On the other hand, stronger corticostriatal projections to both D1 and D2 cells, and a simultaneous decrease in striatal firing thresholds, chosen to mimic a reduction in striatal signal-to-noise ratio, do not lead to the expected rate changes. This accords with the findings of Leblois et al. (2006), but in contrast to that study, we conclude from the experimental literature and our work that dopamine loss often leads to significant changes in firing rates. Note that our results suggest that a combination of reduced corticostriatal connection strengths and striatal firing thresholds of both D1 and D2 populations does not adequately reflect physiological changes upon dopamine loss, but this does not exclude the possibility that dopamine acts as a contrast enhancer (Nicola et al., 2004). This role of dopamine may be mediated by changes in intrinsic properties secondary in importance to changes in synaptic properties (Moyer et al., 2007).

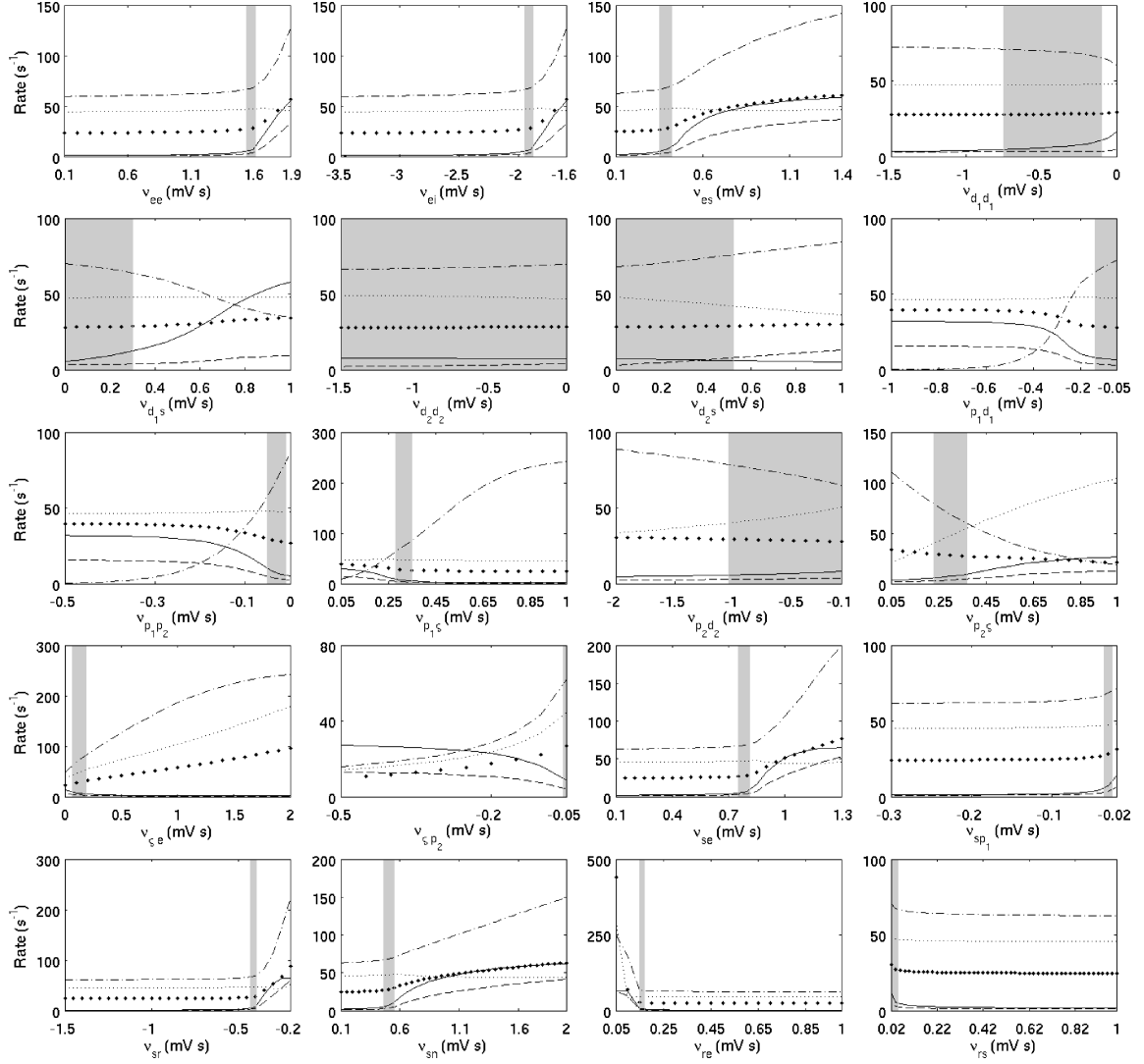


Figure 8: Sensitivity of steady-state firing rates to connection strengths  $\nu_{ab}$ . Shaded regions indicate parameter ranges that yield realistic firing rates in the healthy state for all neuronal populations. Solid,  $\phi_{d_1}$ ; dashed,  $\phi_{d_2}$ ; dash-dotted,  $\phi_{p_1}$ , dotted,  $\phi_{p_2}$ ; large dots,  $\phi_{\varsigma}$ .

(ii) Besides changes in corticostriatal coupling, several other connection strengths and firing thresholds are likely to be altered in PD. Loss of mesocortical dopamine is expected to reduce intracortical excitation and especially inhibition (Gao and Goldman-Rakic, 2003; Gullledge and Jaffe, 2001; Sesack and Bunney, 1989; Thurley et al., 2008; Zhou and Hablitz, 1999). Enhanced enkephalin release may result in weakened lateral inhibition in the GPe (Stanford and Cooper, 1999; Terman et al., 2002), while reduced availability of dynorphin is expected to lower the GPe firing threshold (Ogura and Kita, 2000). Higher levels of extracellular potassium after SNc lesion increase the excitability of the STN (Strauss et al., 2008). In addition, loss of direct dopaminergic innervation stimulates GABA release at striato-GPe terminals, increasing the corresponding connection strength (Floran et al., 1997; Querejeta et al., 2001). Modeling results show that reduced intracortical and intrapallidal inhibition and a lower GPe firing threshold help account for the lack of decrease in cortical rate observed in monkeys and rats with nigrostriatal lesions (Dejean et al., 2008; Goldberg et al., 2002).

(iii) Modeling results suggest that changes in corticostriatal coupling strengths are not solely responsible for substantial increases in STN activity observed in animal models of PD (Bergman et al., 1994; Kreiss et al., 1997; Walters et al., 2007). Reduced intracortical inhibition, a stronger striato-GPe projection, and a lower STN firing threshold all contribute to STN hyperactivity. In the first two cases, the increase in STN activity is associated with a further decrease in GPe rate, whereas a lower STN firing threshold increases both rates. Besides increased excitability, it is also possible that altered inputs from the thalamic parafascicular nucleus (Orioux et al., 2000) and/or the PPN (Breit et al., 2001, 2006; Orioux et al., 2000) play a role in STN hyperactivity. The apparent contribution of the PPN to STN hyperactivity found in these studies is paradoxical, because the PPN receives important inhibitory input from the GPi (Yelnik, 2002), which is overactive in PD. Furthermore, PPN lesions have been shown to cause symptoms resembling PD in primates (Aziz et al., 1998; Kojima et al., 1997). The studies of Orioux et al. (2000) and Breit et al. (2001, 2006) were performed in rats, and the results may not generalize to the human situation, since PD is accompanied by significant neuronal loss from the PPN (Pahapill and Lozano, 2000; Zweig et al., 1989), which is not observed in the rat model. The STN also receives a direct dopaminergic projection, which probably contributes to changes in STN activity in PD (Blandini et al., 2000; Brown et al., 1979; Flores et al., 1999; Hassani et al., 1997; Lavoie et al., 1989). An *in vivo* study in rats suggested that dopamine inhibits STN firing (Campbell et al., 1985), whereas Kreiss et al. (1997) found that dopamine enhanced STN activity in intact animals, but reduced its activity after SNc lesion. However, a predominantly facilitatory effect has been more frequently reported, both in experiments (Loucif et al., 2008; Mintz et al., 1986; Ni et al., 2001b; Zhu et al., 2002), and in a modeling study (Humphries et al., 2006). Therefore it is unlikely that loss of intrinsic dopamine contributes to increased STN firing in PD.

(iv) Our model provides many approximate bounds on connection strengths in the BGTCs, and shows how the strengths of various projections may account for differences in rates between studies. Parameter estimation is an arduous task because the available data do not cover all relevant aspects of the electrophysiology of the basal ganglia, and there are often inconsistencies between studies. However, our main results are sufficiently robust that they hold for a large part of the physiologically realistic range.

When interpreting the above results, a number of qualifications should be taken into account. First, we have necessarily simplified basal ganglia connectivity, ignoring for instance the projections from GPe to striatum and TRN (Gandia et al., 1993; Hazrati and Parent, 1991; Kita et al., 1999), from striatum, STN, and PPN to SNc (Gerfen, 1992; Jiménez-Castellanos and Graybiel, 1989; Lavoie and Parent, 1994), and from thalamus to STN (Gonzalo et al., 2002; Orioux et al., 2000). In addition, the direct dopaminergic innervation from SNc to GPi, GPe, STN, and TRN, which appears to be strongest in GPi (Anaya-Martinez et al., 2006; Jan et al., 2000; Lavoie et al., 1989; Smith et al., 1989), may be incorporated in future studies. Although some of these projections may substantially affect the activity of their targets, their relative influences are difficult to ascertain from the literature. For instance, in addition to its major innervation by the cortex, well-documented reciprocal connections with the thalamic relay nuclei, and inputs from GPe, the TRN receives inputs from diverse brainstem and basal forebrain structures (Cornwall et al., 1990). To keep the model tractable, we have assumed that cortical and thalamic stimuli are the major determinants of TRN activity. Similar arguments hold for the other projections listed above.

Most of our analysis has also been based on the simplifying assumption that each of the basal ganglia nuclei can be treated as a unit in which neurons have common levels of inputs and outputs. However, studies indicate that each nucleus consists of territories with slightly different connectivity patterns. The division of basal ganglia pathways into sensorimotor, associative, and limbic circuits is the most obvious example of this. In addition, parts of the STN have been reported to project specifically to either GPi or GPe (Gonzalo et al., 2002; Parent et al., 1989). Within the GPi, Parent et al. (2001) distinguished between centrally located neurons which terminate in VA, CM-Pf, and PPN, and more peripherally located neurons which innervate the lateral habenula. Moreover, the specific neuronal architectures of the direct and indirect pathways may allow focused excitation of the thalamus via the direct route, and surround inhibition via the indirect route upon cortical stimulation (Haber and Gdowski, 2004). Within the framework provided by our model, the influences of additional projections or more detailed connectivity patterns of the basal ganglia can be assessed with relative ease. The dynamics of the present model is explored in detail in Paper II.

## Acknowledgments

We thank S.C. O'Connor for helpful inputs, and R.T. Gray, C.J. Rennie, P.M. Drysdale, and J.M. Clearwater for useful comments and discussions. This work was supported by the Australian Research Council, an Endeavour International Postgraduate Research Scholarship from the Australian government, and an International Postgraduate Award from the University of Sydney.

## References

- Afsharpour, S., 1985. Topographical projections of the cerebral cortex to the subthalamic nucleus. *J. Comp. Neurol.*, 236, 14–28.
- Aizman, O., Brismar, H., Uhlén, P., Zettergren, E., Levey, A.I., Forsberg, H., Greengard, P., Aperia, A., 2000. Anatomical and physiological evidence for D<sub>1</sub> and D<sub>2</sub> dopamine receptor colocalization in neostriatal neurons. *Nat. Neurosci.*, 3, 226–230.
- Albin, R.L., Young, A.B., Penney, J.B., 1989. The functional anatomy of basal ganglia disorders. *Trends Neurosci.*, 12, 366–375.
- Alexander, G.E., Crutcher, M.D., 1990. Functional architecture of basal ganglia circuits: neural substrates of parallel processing. *Trends Neurosci.*, 13, 266–271.
- Alexander, G.E., DeLong, M.R., Strick, P.L., 1986. Parallel organization of functionally segregated circuits linking basal ganglia and cortex. *Ann. Rev. Neurosci.*, 9, 357–381.
- Anaya-Martinez, V., Martinez-Marcos, A., Martinez-Fong, D., Aceves, J., Erij, D., 2006. Substantia nigra compacta neurons that innervate the reticular thalamic nucleus in the rat also project to striatum or globus pallidus: implications for abnormal motor behavior. *Neuroscience*, 143, 477–486.
- Anderson, M.E., Turner, R.S., 1991. Activity of neurons in cerebellar-receiving and pallidal-receiving areas of the thalamus of the behaving monkey. *J. Neurophysiol.*, 66, 879–893.
- Aosaki, T., Kimura, M., Graybiel, A.M., 1995. Temporal and spatial characteristics of tonically active neurons of the primate's striatum. *J. Neurophysiol.*, 73, 1234–1252.
- Augood, S.J., Emson, P.C., Mitchell, I.J., Boyce, S., Clarke, C.E., Crossman, A.R., 1989. Cellular localisation of enkephalin gene expression in MPTP-treated cynomolgus monkeys. *Mol. Brain Res.*, 6, 85–92.
- Aziz, T.Z., Davies, L., France, S., 1998. The role of descending basal ganglia connections to the brain stem in Parkinsonian akinesia. *Br. J. Neurosurgery*, 12, 245–249.

- Bar-Gad, I., Morris, G., Bergman, H., 2003. Information processing, dimensionality reduction and reinforcement learning in the basal ganglia. *Prog. Neurobiol.*, 71, 439–473.
- Benazzouz, A., Gao, D.M., Ni, Z.G., Piallat, B., Bouali-Benazzouz, R., Benabid, A.L., 2000. Effect of high-frequency stimulation of the subthalamic nucleus on the neuronal activities of the substantia nigra pars reticulata and ventrolateral nucleus of the thalamus in the rat. *Neuroscience*, 99, 289–295.
- Benazzouz, A., Breit, S., Koudsie, A., Pollak, P., Krack, P., Benabid, A.L., 2002. Intraoperative microrecordings of the subthalamic nucleus in Parkinson’s disease. *Mov. Disord.*, 17 (Suppl. 3), S145–S149.
- Bergman, H., Deuschl, G., 2002. Pathophysiology of Parkinson’s disease: from clinical neurology to basic neuroscience and back. *Mov. Disord.*, 17 (Suppl. 3), S28–S40.
- Bergman, H., Wichmann, T., Karmon, B., DeLong, M.R., 1994. The primate subthalamic nucleus. II. Neuronal activity in the MPTP model of parkinsonism. *J. Neurophysiol.*, 72, 507–520.
- Betarbet, R., Greenamyre, J.T., 2004. Regulation of dopamine receptor and neuropeptide expression in the basal ganglia of monkeys treated with MPTP. *Exp. Neurol.*, 189, 393–403.
- Blackwell, K.T., Czubayko, K.T., Plenz, D., 2003. Quantitative estimate of synaptic inputs to striatal neurons during up and down states in vitro. *J. Neurosci.*, 23, 9123–9132.
- Blandini, F., Nappi, G., Tassorelli, C., Martignoni, E., 2000. Functional changes of the basal ganglia circuitry in Parkinson’s disease. *Prog. Neurobiol.*, 62, 63–88.
- Bolam, J.P., Hanley, J.J., Booth, P.A.C., Bevan, M.D., 2000 Synaptic organisation of the basal ganglia *J. Anat.*, 196, 527–542.
- Boraud, T., Bezard, E., Guehl, D., Bioulac, B., Gross, C., 1998. Effects of L-DOPA on neuronal activity of the globus pallidus externalis (GPe) and globus pallidus internalis (GPi) in the MPTP-treated monkey. *Brain Res.*, 787, 157–160.
- Braitenberg, V., Schüz, A., 1998. *Cortex: Statistics and Geometry of Neuronal Connectivity*, second ed. Springer-Verlag, Berlin, Heidelberg, New York.
- Breakspear, M., Roberts, J.A., Terry, J.R., Rodrigues, S., Mahant, N., Robinson, P.A., 2006. A unifying explanation of primary generalized seizures through nonlinear brain modeling and bifurcation analysis. *Cereb. Cortex*, 16, 1296–1313.
- Breit, S., Bouali-Benazzouz, R., Benabid, A.-L., Benazzouz, A., 2001. Unilateral lesion of the nigrostriatal pathway induces an increase of neuronal activity of the pedunculopontine nucleus, which is reversed by the lesion of the subthalamic nucleus in the rat. *Eur. J. Neurosci.*, 14, 1833–1842.
- Breit, S., Lessmann, L., Unterbrink, D., Popa, R.C., Gasser, T., Schulz, J.B., 2006. Lesion of the pedunculopontine nucleus reverses hyperactivity of the subthalamic nucleus and substantia nigra pars reticulata in a 6-hydroxydopamine rat model. *Eur. J. Neurosci.*, 24, 2275–2282.
- Bressloff, P.C., 2001. Traveling fronts and wave propagation failure in an inhomogeneous neural network. *Physica D*, 155, 83–100.
- Bressloff, P.C., Folias, S.E., Prat, A., Li, Y.-X., 2003. Oscillatory waves in inhomogeneous neural media. *Phys. Rev. Lett.*, 91, 178101.1–4.
- Brown, P., 2000. Cortical drives to human muscle: the Piper and related rhythms. *Prog. Neurobiol.*, 60, 97–108.
- Brown, L.L., Makman, M.H., Wolfson, L.I., Dvorkin, B., Warner, C., Katzman, R., 1979. A direct role of dopamine in the rat subthalamic nucleus and adjacent intrapeduncular area. *Science*, 206, 1416–1418.

- Bruno, R.M., Sakmann, B., 2006. Cortex is driven by weak but synchronously active thalamo-cortical synapses. *Science*, 312, 1622–1627.
- Budd, J.M.L., 2004. How much feedback from visual cortex to lateral geniculate nucleus in cat: a perspective. *Visual Neurosci.*, 21, 487–500.
- Burbaud, P., Gross, C., Benazzouz, A., Coussemaeq, M., 1995. Reduction of apomorphine-induced rotational behaviour by subthalamic lesion in 6-OHDA lesioned rats is associated with a normalization of firing rate and discharge patterns of pars reticulata neurons. *Exp. Brain Res.*, 105, 48–58.
- Burns, B.D., 1951. Some properties of isolated cerebral cortex in the unanaesthetized cat. *J. Physiol.*, 112, 156–175.
- Calabresi, P., Centonze, D., Gubellini, P., Marfia, G.A., Pisani, A., Sancesario, G., Bernardi, G., 2000. Synaptic transmission in the striatum: from plasticity to neurodegeneration. *Prog. Neurobiol.*, 61, 231–265.
- Campbell, G.A., Eckardt, M.J., Weight, F.F., 1985. Dopaminergic mechanisms in subthalamic nucleus of rat: analysis using horseradish peroxidase and microiontophoresis. *Brain Res.*, 333, 261–270.
- Carpenter, M.B., 1981. Anatomy of the corpus striatum and brain stem integrating systems. In: *Handbook of Physiology*, vol. 2. American Physiological Society, Bethesda, MD, pp. 947–995.
- Cepeda, C., Colwell, C.S., Itri, J.N., Chandler, S.H., Levine, M.S., 1998. Dopaminergic modulation of NMDA-induced whole cell currents in neostriatal neurons in slices: contribution of calcium conductances. *J. Neurophysiol.*, 79, 82–94.
- Chen, M.-T., Morales, M., Woodward, D.J., Hoffer, B.J., Janak, P.H., 2001. In vivo extracellular recording of striatal neurons in the awake rat following unilateral 6-hydroxydopamine lesions. *Exp. Neurol.* 171, 72–83.
- Cheruel, F., Dormont, J.F., Farin, D., 1996. Activity of neurons of the subthalamic nucleus in relation to motor performance in the cat. *Exp. Brain Res.*, 108, 206–220.
- Chervin, R.D., Pierce, P.A., Connors, B.W., 1988. Periodicity and directionality in the propagation of epileptiform discharges across neocortex. *J. Neurophysiol.*, 60, 1695–1713.
- Clugnet, M.-C., LeDoux, J.E., Morrison, S.F., 1990. Unit responses evoked in the amygdala and striatum by electrical stimulation of the medial geniculate body. *J. Neurosci.*, 10, 1055–1061.
- Cooper, A.J., Stanford, I.M., 2000. Electrophysiological and morphological characteristics of three subtypes of rat globus pallidus neurone in vitro. *J. Physiol.*, 527, 291–304.
- Cornwall, J., Cooper, J.D., Phillipson, O.T., 1990. Projections to the rostral reticular thalamic nucleus in the rat. *Exp. Brain Res.*, 80, 157–171.
- Cox, C.L., Huguenard, J.R., Prince, D.A., 1997. Nucleus reticularis neurons mediate diverse inhibitory effects in thalamus. *Proc. Natl. Acad. Sci. USA*, 94, 8854–8859.
- Day, M., Wang, Z., Ding, J., An, X., Ingham, C.A., Shering, A.F., Wokosin, D., Ilijic, E., Sun, Z., Sampson, A.R., Mugnaini, E., Deutch, A.Y., Sesack, S.R., Arbuthnott, G.W., Surmeier, D.J., 2006. Selective elimination of glutamatergic synapses on striatopallidal neurons in Parkinson disease models. *Nat. Neurosci.*, 9, 2006.
- Dejean, C., Gross, C.E., Bioulac, B., Boraud, T., 2008. Dynamic changes in the cortex-basal ganglia network after dopamine depletion in the rat. *J. Neurophysiol.*, 100, 385–396.
- DeLong, M.R., 1971. Activity of pallidal neurons during movement. *J. Neurophysiol.*, 34, 414–427.
- DeLong, M.R., 1990. Primate models of movement disorders of basal ganglia origin. *Trends Neurosci.*, 13, 281–285.

- DeLong, M.R., Crutcher, M.D., Georgopoulos, A.P., 1983. Relations between movement and single cell discharge in the substantia nigra of the behaving monkey. *J. Neurosci.*, 3, 1599–1606.
- DeLong, M.R., Crutcher, M.D., Georgopoulos, A.P., 1985. Primate globus pallidus and subthalamic nucleus: functional organization. *J. Neurophysiol.*, 53, 530–543.
- Deng, Y.P., Albin, R.L., Penney, J.B., Young, A.B., Anderson, K.D., Reiner, A., 2004. Differential loss of striatal projection systems in Huntington’s disease: a quantitative immunohistochemical study. *J. Chem. Neuroanat.*, 27, 143–164.
- Destexhe, A., Sejnowski, T.J., 2001. *Thalamocortical Assemblies: How Ion Channels, Single Neurons, and Large-Scale Networks Organize Sleep Oscillations*. Oxford University Press, Oxford.
- Destexhe, A., Sejnowski, T.J., 2003. Interactions between membrane conductances underlying thalamocortical slow-wave oscillations. *Physiol. Rev.*, 83, 1401–1453.
- Engber, T.M., Boldry, R.C., Kuo, S., Chase, T.N., 1992. Dopaminergic modulation of striatal neuropeptides: differential effects of D<sub>1</sub> and D<sub>2</sub> receptor stimulation on somatostatin, neuropeptide Y, neurotensin, dynorphin and enkephalin. *Brain Res.*, 581, 261–268.
- Engblom, A.C., Johansen, F.F., Kristiansen, U., 2003. Actions and interactions of extracellular potassium and kainate on expression of 13  $\gamma$ -aminobutyric acid type A receptor subunits in cultured mouse cerebellar granule neurons. *J. Biol. Chem.*, 278, 16543–16550.
- Erişir, A., Van Horn, S.C., Bickford, M.E., Sherman, S.M., 1997. Immunocytochemistry and distribution of parabrachial terminals in the lateral geniculate nucleus of the cat: a comparison with corticogeniculate terminals. *J. Comp. Neurol.*, 377, 535–549.
- Filion, M., Tremblay, L., 1991. Abnormal spontaneous activity of globus pallidus neurons in monkeys with MPTP-induced parkinsonism. *Brain Res.*, 547, 142–151.
- Floran, B., Floran, L., Sierra, A., Aceves, J., 1997. D2 receptor-mediated inhibition of GABA release by endogenous dopamine in the rat globus pallidus. *Neurosci. Lett.*, 237, 1–4.
- Flores, G., Liang, J.J., Martinez-Fong, D., Quirion, R., Aceves, J., Srivastava, L.K., 1999. Expression of dopamine receptors in the subthalamic nucleus of the rat: characterization using reverse transcriptase polymerase chain reaction and autoradiography. *Neuroscience*, 91, 549–556.
- Fujikawa, D.G., Kim, J.S., Daniels, A.H., Alcaraz, A.F., Sohn, T.B., 1996. *In vivo* elevation of extracellular potassium in the rat amygdala increases extracellular glutamate and aspartate and damages neurons. *Neuroscience*, 74, 695–706.
- Gandia, J.A., De Las Heras, S., García, M., Giménez-Amaya, J.M., 1993. Afferent projections to the reticular thalamic nucleus from the globus pallidus and the substantia nigra in the rat. *Brain Res. Bull.*, 32, 351–358.
- Gao, W.-J., Goldman-Rakic, P.S., 2003. Selective modulation of excitatory and inhibitory microcircuits by dopamine. *Proc. Natl. Acad. Sci. USA*, 100, 2836–2841.
- Gaspar, P., Stepniewska, I., Kaas, J.H., 1992. Topography and collateralization of the dopaminergic projections to motor and lateral prefrontal cortex in owl monkeys. *J. Comp. Neurol.*, 325, 1–21.
- Gentet, L.J., Ulrich, D., 2003. Strong, reliable and precise synaptic connections between thalamic relay cells and neurones of the nucleus reticularis in juvenile rats. *J. Physiol.*, 546, 801–811.
- Georgopoulos, A.P., DeLong, M.R., Crutcher, M.D., 1983. Relations between parameters of step-tracking movements and single cell discharge in the globus pallidus and subthalamic nucleus of the behaving monkey. *J. Neurosci.*, 3, 1586–1598.
- Gerfen, C.R., Herkenham, M., Thibault, J., 1987. The neostriatal mosaic: II. Patch- and matrix-directed mesostriatal dopaminergic and non-dopaminergic systems. *J. Neurosci.*, 7, 3915–3934.

- Gerfen, C.R., Engber, T.M., Mahan, L.C., Susel, Z., Chase, T.N., Monsma, F.J. Jr., Sibley, D.R., 1990. D1 and D2 dopamine receptor-regulated gene expression of striatonigral and striatopallidal neurons. *Science*, 250, 1429–1432.
- Gerfen, C.R., 1992. The neostriatal mosaic: multiple levels of compartmental organization. *Trends Neurosci.*, 15, 133–139.
- Gil, Z., Connors, B.W., Amitai, Y., 1999. Efficacy of thalamocortical and intracortical synaptic connections: quanta, innervation, and reliability. *Neuron*, 23, 385–397.
- Gnanalingham, K.K., Milkowski, N.A., Smith, L.A., Hunter, A.J., Jenner, P., Marsden, C.D., 1995. Short and long-term changes in cerebral [ $^{14}\text{C}$ ]-2-deoxyglucose uptake in the MPTP-treated marmoset: relationship to locomotor activity. *J. Neural Transm.*, 101, 65–82.
- Goldberg, J.A., Boraud, T., Maraton, S., Haber, S.N., Vaadia, E., Bergman, H., 2002. Enhanced synchrony among primary motor cortex neurons in the 1-methyl-4-phenyl-1,2,3,6-tetrahydropyridine primate model of Parkinson’s disease. *J. Neurosci.*, 22, 4639–4653.
- Goldman-Rakic, P.S., Selemon, L.D., 1990. New frontiers in basal ganglia research. *Trends Neurosci.*, 13, 241–244.
- Golomb, D., Amitai, Y., 1997. Propagating neuronal discharges in neocortical slices: Computational and experimental study. *J. Neurophysiol.*, 78, 1199–1211.
- Golshani, P., Liu, X.-B., Jones, E.G., 2001. Differences in quantal amplitude reflect GluR4-subunit number at corticothalamic synapses on two populations of thalamic neurons. *Proc. Natl. Acad. Sci.*, 98, 4172–4177.
- Gonzalo, N., Lanciego, J.L., Castle, M., Vázquez, A., Erro, E., Obeso, J.A., 2002. The parafascicular thalamic complex and basal ganglia circuitry: further complexity to the basal ganglia model. *Thal. Rel. Syst.*, 1, 341–348.
- Granseth, B., Lindström, S., 2003. Unitary EPSCs of corticogeniculate fibers in the rat dorsal lateral geniculate nucleus in vitro. *J. Neurophysiol.*, 89, 2952–2960.
- Gray, J.A., Feldon, J., Rawlins, J.N.P., 1991. The neuropsychology of schizophrenia. *Behav. Brain Sci.*, 14, 1–19.
- Graybiel, A.M., 1990. Neurotransmitters and neuromodulators in the basal ganglia. *Trends Neurosci.*, 13, 244–254.
- Groves, P.M., Garcia-Munoz, M., Linder, J.C., Manley, M.S., Martone, M.E., Young, S.J., 1995. Elements of the intrinsic organization and information processing in the neostriatum. In: Houk, J., Davis, J., Beiser, D. (Eds.), *Models of Information Processing in the Basal Ganglia*. MIT Press, Cambridge, Massachusetts, pp. 51–96.
- Gullledge, A.T., Jaffe, D.B., 2001. Multiple effects of dopamine on layer V pyramidal cell excitability in rat prefrontal cortex. *J. Neurophysiol.*, 86, 586–595.
- Gurney, K., Prescott, T.J., Redgrave, P., 2001a. A computational model of action selection in the basal ganglia. I. A new functional anatomy. *Biol. Cybern.*, 84, 401–410.
- Gurney, K., Prescott, T.J., Redgrave, P., 2001b. A computational model of action selection in the basal ganglia. II. Analysis and simulation of behaviour. *Biol. Cybern.*, 84, 411–423.
- Haber, S.N., Gdowski, M.J., 2004. The basal ganglia. In: Paxinos, G., Mai, J. (Eds.), *The Human Nervous System*. Elsevier, pp. 676–738.
- Haber, S.N., Fudge, J.L., McFarland, N.R., 2000. Striatonigrostriatal pathways in primates form an ascending spiral from the shell to the dorsolateral striatum. *J. Neurosci.*, 20, 2369–2382.

- Hamada, I., DeLong, M.R., 1992. Excitotoxic acid lesions of the primate subthalamic nucleus result in reduced pallidal neuronal activity during active holding. *J. Neurophysiol.*, 68, 1859–1866.
- Hanley, J.J., Bolam, J.P., 1997. Synaptology of the nigrostriatal projection in relation to the compartmental organization of the neostriatum in the rat. *Neuroscience*, 81, 353–370.
- Hashimoto, T., Elder, C.M., Okun, M.S., Patrick, S.K., Vitek, J.L., 2003. Stimulation of the subthalamic nucleus changes the firing pattern of pallidal neurons. *J. Neurosci.*, 23, 1916–1923.
- Hassani, O.-K., Mouroux, M., Féger, J., 1996. Increased subthalamic neuronal activity after nigral dopaminergic lesion independent of disinhibition via the globus pallidus. *Neuroscience*, 72, 105–115.
- Hassani, O.-K., François, C., Yelnik, J., Féger, J., 1997. Evidence for a dopaminergic innervation of the subthalamic nucleus in the rat. *Brain Res.*, 749, 88–94.
- Hazrati, L.-N., Parent, A., 1991. Projection from the external pallidum to the reticular thalamic nucleus in the squirrel monkey. *Brain Res.*, 550, 142–146.
- Hazrati, L.-N., Parent, A., Mitchell, S., Haber, S.N., 1990. Evidence for interconnections between the two segments of the globus pallidus in primates: a PHA-L anterograde tracing study. *Brain Res.*, 533, 171–175.
- Heimer, G., Bar-Gad, I., Goldberg, J.A., Bergman, H., 2002. Dopamine replacement therapy reverses abnormal synchronization of pallidal neurons in the 1-methyl-4-phenyl-1,2,3,6-tetrahydropyridine primate model of Parkinsonism. *J. Neurosci.*, 22, 7850–7855.
- Hernández-López, S., Bargas, J., Surmeier, D.J., Reyes, A., Galarraga, E., 1997. D<sub>1</sub> receptor activation enhances discharge in neostriatal medium spiny neurons by modulating an L-type Ca<sup>2+</sup> conductance. *J. Neurosci.*, 17, 3334–3342.
- Hersch, S.M., Ciliax, B.J., Gutekunst, C.-A., Rees, H.D., Heilman, C.J., Yung, K.K.L., Bolam, J.P., Ince, E., Yi, H., Levey, A.I., 1995. Electron microscopic analysis of D1 and D2 dopamine receptor proteins in the dorsal striatum and their synaptic relationships with motor corticostriatal afferents. *J. Neurosci.*, 15, 5222–5237.
- Hestrin, S., Sah, P., Nicoll, R.A., 1990. Mechanisms generating the time course of dual component excitatory synaptic currents recorded in hippocampal slices. *Neuron*, 5, 247–253.
- Hollerman, J.R., Grace, A.A., 1992. Subthalamic nucleus cell firing in the 6-OHDA-treated rat: basal activity and response to haloperidol. *Brain Res.*, 590, 291–299.
- Hsu, K.-S., Huang, C.-C., Yang, C.-H., Gean, P.-W., 1995. Presynaptic D<sub>2</sub> dopaminergic receptors mediate inhibition of excitatory synaptic transmission in rat neostriatum. *Brain Res.*, 690, 264–268.
- Hu, X.-T., Wachtel, S.R., Galloway, M.P., White, F.J., 1990. Lesions of the nigrostriatal dopamine projection increase the inhibitory effects of D<sub>1</sub> and D<sub>2</sub> dopamine agonists on caudate-putamen neurons and relieve D<sub>2</sub> receptors from the necessity of D<sub>1</sub> receptor stimulation. *J. Neurosci.*, 10, 2318–2329.
- Hu, X.-T., White, F.J., 1997. Dopamine enhances glutamate-induced excitation of rat striatal neurons by cooperative activation of D<sub>1</sub> and D<sub>2</sub> class receptors. *Neurosci. Lett.*, 224, 61–65.
- Humphries, M.D., Gurney, K.N., 2001. A pulsed neural network model of bursting in the basal ganglia. *Neural Networks*, 14, 845–863.
- Humphries, M.D., Stewart, R.D., Gurney, K.N., 2006. A physiologically plausible model of action selection and oscillatory activity in the basal ganglia. *J. Neurosci.*, 26, 12921–12942.

- Hutchison, W.D., Lozano, A.M., Davis, K.D., Saint-Cyr, J.A., Lang, A.E., Dostrovsky, J.O., 1994. Differential neuronal activity in segments of globus pallidus in Parkinson's disease patients. *NeuroReport*, 5, 1533–1537.
- Hutchison, W.D., Allan, R.J., Opitz, H., Levy, R., Dostrovsky, J.O., Lang, A.E., Lozano, A.M., 1998. Neurophysiological identification of the subthalamic nucleus in surgery for Parkinson's disease. *Ann. Neurol.*, 44, 622–628.
- Ilinsky, I.A., Tourtellotte, W.G., Kultas-Ilinsky, K., 1993. Anatomical distinctions between the two basal ganglia afferent territories in the primate motor thalamus. *Stereotact. Funct. Neurosurg.*, 60, 62–69.
- Inase, M., Li, B.-M., Tanji, J., 1997. Dopaminergic modulation of neuronal activity in the monkey putamen through D1 and D2 receptors during a delayed Go/Nogo task. *Exp. Brain Res.*, 117, 207–218.
- Jackson, S.R., Marrocco, R., Posner, M.I., 1994. Networks of anatomical areas controlling visuospatial attention. *Neural Networks*, 7, 925–944.
- Jan, C., François, C., Tandé, D., Yelnik, J., Tremblay, L., Agid, Y., Hirsch, E., 2000. Dopaminergic innervation of the pallidum in the normal state, in MPTP-treated monkeys and in parkinsonian patients. *Eur. J. Neurosci.*, 12, 4525–4535.
- Jenkins, I.H., Fernandez, W., Playford, E.D., Lees, A.J., Frackowiak, R.S.J., Passingham, R.E., Brooks, D.J., 1992. Impaired activation of the supplementary motor area in Parkinson's disease is reversed when akinesia is treated with apomorphine. *Ann. Neurol.*, 32, 749–757.
- Jiménez-Castellanos, J., Graybiel, A.M., 1989. Compartmental origins of striatal efferent projections in the cat. *Neuroscience*, 32, 297–321.
- Jirsa, V.K., Haken, H., 1996. Field theory of electromagnetic brain activity. *Phys. Rev. Lett.*, 77, 960–963.
- Jirsa, V.K., Haken, H., 1997. A derivation of a macroscopic field theory of the brain from the quasi-microscopic neural dynamics. *Physica D*, 99, 503–526.
- Joyce, J.N., Lexow, N., Bird, E., Winokur, A., 1988. Organization of dopamine D1 and D2 receptors in human striatum: receptor autoradiographic studies in Huntington's disease and schizophrenia. *Synapse*, 2, 546–557.
- Kawaguchi, Y., Wilson, C.J., Augood, S.J., Emson, P.C., 1995. Striatal interneurons: chemical, physiological and morphological characterization. *Trends Neurosci.*, 18, 527–535.
- Kerr, C.C. and Rennie, C.J., Robinson, P.A., 2008. Physiology-based modeling of cortical auditory evoked potentials. *Biol. Cybern.*, 98, 171–184.
- Kim, R., Nakano, K., Jayaraman, A., Carpenter, M.B., 1976. Projections of the globus pallidus and adjacent structures: an autoradiographic study in the monkey. *J. Comp. Neurol.*, 169, 263–290.
- Kimura, M., Rajkowski, J., Evarts, E., 1984. Tonicly discharging putamen neurons exhibit set-dependent responses. *Proc. Natl. Acad. Sci. USA*, 81, 4998–5001.
- Kimura, M., Kato, M., Shimazaki, H., Watanabe, K., Matsumoto, N., 1996. Neural information transferred from the putamen to the globus pallidus during learned movement in the monkey. *J. Neurophysiol.*, 76, 3771–3786.
- Kish, L.J., Palmer, M.R., Gerhardt, G.A., 1999. Multiple single-unit recordings in the striatum of freely moving animals: effects of apomorphine and D-amphetamine in normal and unilateral 6-hydroxydopamine-lesioned rats. *Brain Res.*, 833, 58–70.

- Kita, H., 1994. Parvalbumin-immunopositive neurons in rat globus pallidus: a light and electron microscopic study. *Brain Res.*, 657, 31–41.
- Kita, H., 2001. Neostriatal and globus pallidus stimulation induced inhibitory postsynaptic potentials in entopeduncular neurons in rat brain slice preparations. *Neuroscience*, 105, 871–879.
- Kita, H., Chang, H., Kitai, S., 1983. Pallidal inputs to subthalamus: intracellular analysis. *Brain Res.*, 264, 255–265.
- Kita, H., Tokuno, H., Nambu, A., 1999. Monkey globus pallidus external segment neurons projecting to the neostriatum. *NeuroReport*, 10, 1467–1472.
- Kita, H., Nambu, A., Kaneda, K., Tachibana, Y., Takada, M., 2004. Role of ionotropic glutamatergic and GABAergic inputs on the firing activity of neurons in the external pallidum in awake monkeys. *J. Neurophysiol.*, 92, 3069–3084.
- Kiyatkin, E.A., Rebec, G.V., 1996. Dopaminergic modulation of glutamate-induced excitations of neurons in the neostriatum and nucleus accumbens of awake, unrestrained rats. *J. Neurophysiol.*, 75, 142–153.
- Kiyatkin, E.A., Rebec, G.V., 1999. Striatal neuronal activity and responsiveness to dopamine and glutamate after selective blockade of D1 and D2 dopamine receptors in freely moving rats. *J. Neurosci.*, 19, 3594–3609.
- Kojima, J., Yamaji, Y., Matsumura, M., Nambu, A., Inase, M., Tokuno, H., Takada, M., Imai, H., 1997. Excitotoxic lesions of the pedunculopontine tegmental nucleus produce contralateral hemiparkinsonism in the monkey. *Neurosci. Lett.*, 226, 111–114.
- Koós, T., Tepper, J.M., 1999 Inhibitory control of neostriatal projection neurons by GABAergic interneurons. *Nat. Neurosci.*, 2, 467–472.
- Kreiss, D.S., Mastropietro, C.W., Rawji, S.S., Walters, J.R., 1997. The response of subthalamic nucleus neurons to dopamine receptor stimulation in a rodent model of Parkinson’s disease. *J. Neurosci.*, 17, 6807–6819.
- Lavoie, B., Parent, A., 1994. Pedunculopontine nucleus in the squirrel monkey: projections to the basal ganglia as revealed by anterograde tract-tracing methods. *J. Comp. Neurol.*, 344, 210–231.
- Lavoie, B., Smith, Y., Parent, A., 1989. Dopaminergic innervation of the basal ganglia in the squirrel monkey as revealed by tyrosine hydroxylase immunohistochemistry. *J. Comp. Neurol.*, 289, 36–52.
- Leblois, A., Boraud, T., Meissner, W., Bergman, H., Hansel, D., 2006. Competition between feedback loops underlies normal and pathological dynamics in the basal ganglia. *J. Neurosci.*, 26, 3567–3583.
- Le Moine, C., Bloch, B., 1995. D1 and D2 dopamine receptor gene expression in the rat striatum: sensitive cRNA probes demonstrate prominent segregation of D1 and D2 mRNAs in distinct neuronal populations of the dorsal and ventral striatum. *J. Comp. Neurol.*, 355, 418–426.
- Lester, J., Fink, S., Aronin, N., DiFiglia, M., 1993. Colocalization of D<sub>1</sub> and D<sub>2</sub> dopamine receptor mRNAs in striatal neurons. *Brain Res.*, 621, 106–110.
- Lévesque, M., Parent, A., 2005. The striatofugal fiber system in primates: a reevaluation of its organization based on single-axon tracing studies. *Proc. Natl. Acad. Sci. USA*, 102, 11888–11893.
- Levine, M.S., Li, Z., Cepeda, C., Cromwell, H.C., Altemus, K.L., 1996. Neuromodulatory actions of dopamine on synaptically-evoked neostriatal responses in slices. *Synapse*, 24, 65–78.

- Levy, R., Hutchison, D., Lozano, A.M., Dostrovsky, J.O., 2000. High-frequency synchronization of neuronal activity in the subthalamic nucleus of parkinsonian patients with limb tremor. *J. Neurosci.*, 20, 7766–7775.
- Liu, X.-B., Jones, E.G., 1999. Predominance of corticothalamic synaptic inputs to thalamic reticular nucleus neurons in the rat. *J. Comp. Neurol.*, 414, 67–79.
- Lo, C.-C., Wang, X.-J., 2006. Cortico-basal ganglia circuit mechanism for a decision threshold in reaction time tasks. *Nat. Neurosci.*, 9, 956–963.
- Lopes da Silva, F.H., Storm van Leeuwen, W., 1978. The cortical alpha rhythm in dog: the depth and surface profile of phase. In: Brazier, M.A.B., Petsche, H. (Eds.), *Architectonics of the Cerebral Cortex*. Raven, New York, pp. 319–333.
- Loucif, A.J.C., Woodhall, G.L., Sehrlirli, U.S., Stanford, I.M., 2008. Depolarisation and suppression of burst firing activity in the mouse subthalamic nucleus by dopamine D1/D5 receptor activation of a cyclic-nucleotide gated non-specific cation conductance. *Neuropharmacology*, 55, 94–105.
- MacLeod, N.K., Ryman, A., Arbuthnott, G.W., 1990. Electrophysiological properties of nigrothalamic neurons after 6-hydroxydopamine lesions in the rat. *Neuroscience*, 38, 447–456.
- Magill, P.J., Bolam, J.P., Bevan, M.D., 2001. Dopamine regulates the impact of the cerebral cortex on the subthalamic nucleus-globus pallidus network. *Neuroscience*, 106, 313–330.
- Magnin, M., Morel, A., Jeanmonod, D., 2000. Single-unit analysis of the pallidum, thalamus and subthalamic nucleus in parkinsonian patients. *Neuroscience*, 96, 549–564.
- Mallet, N., Ballion, B., Le Moine, C., Gonon, F., 2006. Cortical inputs and GABA interneurons imbalance projection neurons in the striatum of parkinsonian rats. *J. Neurosci.*, 26, 3884–3875.
- Maneuf, Y.P., Mitchell, I.J., Crossman, A.R., Brotchie, J.M., 1994. On the role of enkephalin cotransmission in the GABAergic striatal efferents to the globus pallidus. *Exp. Neurol.*, 125, 65–71.
- Maurice, N., Deniau, J.-M., Glowinski, J., Thierry, A.-M., 1998. Relationships between the prefrontal cortex and the basal ganglia in the rat: physiology of the corticosubthalamic circuits. *J. Neurosci.*, 18, 9539–9546.
- McCormick, D.A., Connors, B.W., Lighthall, J.W., Prince, D.A., 1985. Comparative electrophysiology of pyramidal and sparsely spiny stellate neurons of the neocortex. *J. Neurophysiol.*, 54, 782–806.
- McFarland, N.R., Haber, S.N., 2000. Convergent inputs from thalamic motor nuclei and frontal cortical areas to the dorsal striatum in the primate. *J. Neurosci.*, 20, 3798–3813.
- Meador-Woodruff, J.H., Mansour, A., Healy, D.J., Kuehn, R., Zhou, Q.J., Bunzow, J.R., Akil, H., Civelli, O., Watson, S.J.Jr., 1991. Comparison of the distributions of D1 and D2 dopamine receptor mRNAs in rat brain. *Neuropsychopharmacology*, 5, 231–242.
- Merello, M., Balej, J., Delfino, M., Cammarota, A., Betti, O., Leiguarda, R., 1999. Apomorphine induces changes in GPi spontaneous outflow in patients with Parkinson’s disease. *Mov. Disord.*, 14, 45–49.
- Mintz, I., Hammond, C., Féger, J., 1986. Excitatory effect of iontophoretically applied dopamine on identified neurons of the rat subthalamic nucleus. *Brain Res.*, 375, 172–175.
- Mitchell, I.J., Cross, A.J., Sambrook, M.A., Crossman, A.R., 1986. Neural mechanisms mediating 1-methyl-4-phenyl-1,2,3,6-tetrahydropyridine (MPTP)-induced parkinsonism in the monkey: relative contributions of the striatopallidal and striatonigral pathways as suggested by 2-deoxyglucose uptake. *Neurosci. Lett.*, 63, 61–65.

- Miwa, H., Nishi, K., Fuwa, T., Mizuno, Y., 1998. Postural effects of unilateral blockade of glutamatergic neurotransmission in the subthalamic nucleus on haloperidol-induced akinesia in rats. *Neurosci. Lett.*, 252, 167–170.
- Molnar, G.F., Pilliar, A., Lozano, A.M., Dostrovsky, J.O., 2005. Differences in neuronal firing rates in pallidal and cerebellar receiving areas of thalamus in patients with Parkinson's disease, essential tremor, and pain. *J. Neurophysiol.*, 93, 3094–3101.
- Monchi, O., Petrides, M., Doyon, J., Postuma, R.B., Worsley, K., Dagher, A., 2004. Neural bases of set-shifting deficits in Parkinson's disease. *J. Neurosci.*, 24, 702–710.
- Monchi, O., Petrides, M., Mejia-Constain, B., and Strafella, A.P., 2007. Cortical activity in Parkinson's disease during executive processing depends on striatal involvement. *Brain*, 130, 233–244.
- Moyer, J.T., Wolf, J.A., Finkel, L.H., 2007. Effects of dopaminergic modulation on the integrative properties of the ventral striatal medium spiny neuron. *J. Neurophysiol.*, 98, 3731–3748.
- Nadjar, A., Brotchie, J.M., Guigoni, C., Li, Q., Zhou, S.-B., Wang, G.-J., Ravenscroft, P., Georges, F., Crossman, A.R., Bezard, E., 2006. Phenotype of striatofugal medium spiny neurons in parkinsonian and dyskinetic nonhuman primates: a call for a reappraisal of the functional organization of the basal ganglia. *J. Neurosci.*, 26, 8653–8661.
- Nakanishi, H., Kita, H., Kitai, S.T., 1987. Electrical membrane properties of rat subthalamic neurons in an in vitro slice preparation. *Brain Res.*, 437, 35–44.
- Nakanishi, H., Kita, H., Kitai, S.T., 1990. Intracellular study of rat entopeduncular nucleus neurons in an in vitro slice preparation: electrical membrane properties. *Brain Res.*, 527, 81–88.
- Nambu, A., Llinás, R., 1994. Electrophysiology of globus pallidus neurons in vitro. *J. Neurophysiol.*, 72, 1127–1139.
- Nambu, A., Llinás, R., 1997. Morphology of globus pallidus neurons: its correlation with electrophysiology in guinea pig brain slices. *J. Comp. Neurol.*, 377, 85–94.
- Nambu, A., Yoshida, S., Jinnai, K., 1988. Projection on the motor cortex of thalamic neurons with pallidal input in the monkey. *Exp. Brain Res.*, 71, 658–662.
- Nambu, A., Takada, M., Inase, M., Tokuno, H., 1996. Dual somatotopical representations in the primate subthalamic nucleus: evidence for ordered but reversed body-map transformations from the primary motor cortex and the supplementary motor area. *J. Neurosci.*, 16, 2671–2683.
- Nambu, A., Tokuno, H., Inase, M., Takada, M., 1997. Corticosubthalamic input zones from forelimb representations of the dorsal and ventral divisions of the premotor cortex in the macaque monkey: comparison with the input zones from the primary motor cortex and the supplementary motor area. *Neurosci. Lett.*, 239, 13–16.
- Nambu, A., Tokuno, H., Hamada, I., Kita, H., Imanishi, M., Akazawa, T., Ikeuchi, Y., Hasegawa, N., 2000. Excitatory cortical inputs to pallidal neurons via the subthalamic nucleus in the monkey. *J. Neurophysiol.*, 84, 289–300.
- Ni, Z.-G., Bouali-Benazzouz, R., Gao, D.-M., Benabid, A.-L., Benazzouz, A., 2001a. Time-course of changes in firing rates and firing patterns of subthalamic nucleus neuronal activity after 6-OHDA-induced dopamine depletion in rats. *Brain Res.*, 899, 142–147.
- Ni, Z.-G., Bouali-Benazzouz, R., Gao, D.-M., Benabid, A.-L., Benazzouz, A., 2001b. Intrastriatal injection of 6-hydroxydopamine induces changes in the firing rate and pattern of subthalamic nucleus neurons in the rat. *Synapse*, 40, 145–153.
- Nicola, S.M., Malenka, R.C., 1998. Modulation of synaptic transmission by dopamine and norepinephrine in ventral but not dorsal striatum. *J. Neurophysiol.*, 79, 1768–1776.

- Nicola, S.M., Surmeier, D.J., Malenka, R.C., 2000. Dopaminergic modulation of neuronal excitability in the striatum and nucleus accumbens. *Ann. Rev. Neurosci.*, 23, 185–215.
- Nicola, S.M., Hopf, F.W., Hjelmstad, G.O., 2004. Contrast enhancement: a physiological effect of striatal dopamine? *Cell Tissue Res.*, 318, 93–106.
- Nowak, L.G., Bullier, J., 1997. The timing of information transfer in the visual system. In: Rockland, K., Kaas, J., Peters, A. (Eds.), *Cerebral Cortex*, vol. 12. Plenum Press, New York, pp. 205–241.
- Nunez, P.L., 1974. Wave-like properties of the alpha rhythm. *IEEE Trans. Biomed. Eng.*, 21, 473–483.
- Nunez, P.L., 1995. *Neocortical Dynamics and Human EEG Rhythms*. Oxford University Press, Oxford.
- O'Connor, S.C., Robinson, P.A., Chiang, A.K.I., 2002. Wave-number spectrum of electroencephalographic signals. *Phys. Rev. E*, 66, 061905.1–061905.12.
- O'Donnell, P., 2003. Dopamine gating of forebrain neural ensembles. *Eur. J. Neurosci.*, 17, 429–435.
- Ogura, M., Kita, H., 2000. Dynorphin exerts both postsynaptic and presynaptic effects in the globus pallidus of the rat. *J. Neurophysiol.*, 83, 3355–3376.
- Orioux, G., François, C., Féger, J., Yelnik, J., Vila, M., Ruberg, M., Agid, Y., Hirsch, E.C., 2000. Metabolic activity of excitatory parafascicular and pedunculopontine inputs to the subthalamic nucleus in a rat model of Parkinson's disease. *Neuroscience*, 97, 79–88.
- Pahapill, P.A., Lozano, A.M., 2000. The pedunculopontine nucleus and Parkinson's disease. *Brain*, 123, 1767–1783.
- Palombo, E., Porrino, L.J., Bankiewicz, K.S., Crane, A.M., Kopin, I.J., Sokoloff, L., 1988. Administration of MPTP acutely increase glucose utilization in the substantia nigra of primates. *Brain Res.*, 453, 227–234.
- Pan, H.S., Walters, J.R., 1988. Unilateral lesion of the nigrostriatal pathway decreases the firing rate and alters the firing pattern of globus pallidus neurons in the rat. *Synapse*, 2, 650–656.
- Parent, A., 1990. Extrinsic connections of the basal ganglia. *Trends Neurosci.*, 13, 254–258.
- Parent, A., Hazrati, L.-N., 1995. Functional anatomy of the basal ganglia. II. The place of subthalamic nucleus and external pallidum in basal ganglia circuitry. *Brain Res. Rev.*, 20, 128–154.
- Parent, A., Smith, Y., Fillion, M., Dumas, J., 1989. Distinct afferents to internal and external pallidal segments in the squirrel monkey. *Neurosci. Lett.*, 96, 140–144.
- Parent, M., Levesque, M., Parent, A., 2001. Two types of projection neurons in the internal pallidum of primates: single-axon tracing and three-dimensional reconstruction. *J. Comp. Neurol.*, 439, 162–175.
- Peckys, D., Landwehrmeyer, G.B., 1999. Expression of mu, kappa, and delta opioid receptor messenger RNA in the human CNS: a <sup>33</sup>P *in situ* hybridization study. *Neuroscience*, 88, 1093–1135.
- Percheron, G., Yelnik, J., François, C., 1984. A Golgi analysis of the primate globus pallidus. III. Spatial organization of the striato-pallidal complex. *J. Comp. Neurol.*, 227, 214–227.
- Pessiglione, M., Guehl, D., Rolland, A.-S., François, C., Hirsch, E.C., Féger, J., 2005. Thalamic neuronal activity in dopamine-depleted primates: evidence for a loss of functional segregation within basal ganglia circuits. *J. Neurosci.*, 25, 1523–1531.

- Peters, A., Payne, B.R., 1993. Numerical relationships between geniculocortical afferents and pyramidal cell modules in cat primary visual cortex. *Cereb. Cortex*, 3, 69–78.
- Plenz, D., 2003. When inhibition goes *incognito*: feedback interaction between spiny projection neurons in striatal function. *Trends Neurosci.*, 26, 436–443.
- Prechtl, J.C., Cohen, L.B., Pesaran, B., Mitra, P.P., Kleinfeld, D., 1997. Visual stimuli induce waves of electrical activity in turtle cortex. *Proc. Natl. Acad. Sci. USA*, 94, 7621–7626.
- Querejeta, E., Delgado, A., Valdiosera, R., Erlij, D., Aceves, J., 2001. Intrapallidal  $D_2$  dopamine receptors control globus pallidus neurons activity in the rat. *Neurosci. Lett.*, 300, 79–82.
- Raeva, S.N., Lukashev, A.O., 1987. Characteristics of background unit activity in the nucleus reticularis of the human thalamus. *Neurophysiology*, 19, 335–343.
- Ragsdale, C.W.Jr., Graybiel, A.M., 1988. Multiple patterns of striatal innervation in the cat. In: Bentivoglio, M., Spreafico, R. (Eds.), *Cellular Thalamic Mechanisms*. Elsevier, Amsterdam, pp. 261–267.
- Raynor, K., Kong, H., Mestek, A., Bye, L.S., Tian, M., Liu, J., Yu, L., Reisine, T., 1995. Characterization of the cloned human  $\mu$  opioid receptor. *J. Pharmacol. Exp. Therap.*, 272, 423–428.
- Reiner, A., Albin, R.L., Anderson, K.D., D’Amato, C.J., Penney, J.B., Young, A.B., 1988. Differential loss of striatal projections neurons in Huntington’s disease. *Proc. Natl. Acad. Sci. USA*, 85, 5733–5737.
- Rennie, C.J., Robinson, P.A., Wright, J.J., 1999. Effects of local feedback on dispersion of electrical waves in the cerebral cortex. *Phys. Rev. E*, 59, 3320–3329.
- Rennie, C.J., Wright, J.J., Robinson, P.A., 2000. Mechanisms of cortical electrical activity and emergence of gamma rhythm. *J. Theor. Biol.*, 205, 17–35.
- Ridding, M.C., Inzelberg, R., Rothwell, J.C., 1995. Changes in excitability of motor cortical circuitry in patients with Parkinson’s disease. *Ann. Neurol.*, 37, 181–188.
- Roberts, J.A., Robinson, P.A., 2008. Modeling absence seizure dynamics: Implications for basic mechanisms and measurement of thalamocortical and corticothalamic latencies. *J. Theor. Biol.*, 253, 189–201.
- Robinson, P.A., 2003. Neurophysical theory of coherence and correlations of electroencephalographic signals. *J. Theor. Biol.*, 222, 163–175.
- Robinson, P.A., Rennie, C.J., Wright, J.J., 1997. Propagation and stability of waves of electrical activity in the cerebral cortex. *Phys. Rev. E*, 56 (1), 826–840.
- Robinson, P.A., Rennie, C.J., Wright, J.J., Bahramali, H., Gordon, E., Rowe, D.L., 2001a. Prediction of electroencephalographic spectra from neurophysiology. *Phys. Rev. E*, 63, 021903.1–021903.18.
- Robinson, P.A., Loxley, P.N., O’Connor, S.C., Rennie, C.J., 2001b. Modal analysis of corticothalamic dynamics, electroencephalographic spectra, and evoked potentials. *Phys. Rev. E*, 63, 041909.1–041909.13.
- Robinson, P.A., Rennie, C.J., Rowe, D.L., 2002. Dynamics of large-scale brain activity in normal arousal states and epileptic seizures. *Phys. Rev. E*, 65, 041924.1–041924.9.
- Robinson, P.A., Rennie, C.J., Rowe, D.L., O’Connor, S.C., Wright, J.J., Gordon, E., Whitehouse, R. W., 2003a. Neurophysical modeling of brain dynamics. *Neuropsychopharmacology*, 28 (Suppl. 1), 74–79.
- Robinson, P.A., Rennie, C.J., Rowe, D.L., O’Connor, S.C., 2004. Estimation of multiscale neurophysiologic parameters by electroencephalographic means. *Hum. Brain Mapp.*, 23, 53–72.

- Robinson, P.A., Rennie, C.J., Rowe, D.L., O'Connor, S.C., Gordon, E., 2005. Multiscale brain modelling. *Phil. Trans. R. Soc. B*, 360, 1043–1050.
- Robledo, P., Feger, J., 1991. Acute monoaminergic depletion in the rat potentiates the excitatory effect of the subthalamic nucleus in the substantia nigra pars reticulata but not in the pallidal complex. *J. Neural Transm.*, 86, 115–126.
- Rohlf, A., Nikkah, G., Rosenthal, C., Rundfeldt, C., Brandis, A., Samii, M., Löscher, W., 1997. Hemispheric asymmetries in spontaneous firing characteristics of substantia nigra pars reticulata neurons following a unilateral 6-hydroxydopamine lesion of the rat nigrostriatal pathway. *Brain Res.*, 761, 352–356.
- Rolland, A.-S., Herrero, M.-T., Garcia-Martinez, V., Ruberg, M., Hirsch, E.C., François, C., 2007. Metabolic activity of cerebellar and basal ganglia-thalamic neurons is reduced in parkinsonism. *Brain*, 130, 265–275.
- Rubin, J.E., Terman, D., 2004. High frequency stimulation of the subthalamic nucleus eliminates pathological thalamic rhythmicity in a computational model. *J. Comp. Neurosci.*, 16, 211–235.
- Rubino, D., Robbins, K.A., Hatsopoulos, N.G., 2006. Propagating waves mediate information transfer in the motor cortex. *Nat. Neurosci.*, 9, 1549–1557.
- Sadikot, A.F., Parent, A., Smith, Y., Bolam, J.P., 1992. Efferent connections of the centromedian and parafascicular thalamic nuclei in the squirrel monkey: a light and electron microscopic study of the thalamostriatal projection in relations to striatal heterogeneity. *J. Comp. Neurol.*, 320, 228–242.
- Salenius, S., Avikainen, S., Kaakola, S., Hari, R., Brown, P., 2002. Defective cortical drive to muscle in Parkinson's disease and its improvement with levodopa. *Brain*, 125, 491–500.
- Sato, F., Lavallée, P., Lévesque, M., Parent, A., 2000. Single-axon tracing study of neurons of the external segment of the globus pallidus in primate. *J. Comp. Neurol.*, 417, 17–31.
- Schiff, S.J., Huang, X., Wu, J.-Y., 2007. Dynamical evolution of spatiotemporal patterns in mammalian middle cortex. *Phys. Rev. Lett.*, 98, 178102.1–4.
- Schneider, J.S., Rothblat, D.S., 1996. Alterations in intralaminar and motor thalamic physiology following nigrostriatal dopamine depletion. *Brain Res.*, 742, 25–33.
- Schultz, W., 1986. Activity of pars reticulata neurons of monkey substantia nigra in relation to motor, sensory, and complex events. *J. Neurophysiol.*, 55, 660–677.
- Sesack, S.R., Bunney, B.S., 1989. Pharmacological characterization of the receptor mediating electrophysiological responses to dopamine in the rat medial prefrontal cortex: A microiontophoretic study. *J. Pharmacol. Exp. Therap.*, 248, 1323–1333.
- Shen, K.-Z., Johnson, S.W., 2002. Presynaptic modulation of synaptic transmission by opioid receptor in rat subthalamic nucleus *in vitro*, 2002. *J. Physiol.*, 541, 219–230.
- Sherman, S.M., Guillery, R.W., 2002. The role of the thalamus in the flow of information to the cortex. *Phil. Trans. R. Soc. Lond. B*, 357, 1695–1708.
- Shink, E., Smith, Y., 1995. Differential synaptic innervation of neurons in the internal and external segments of the globus pallidus by the GABA- and glutamate-containing terminals in the squirrel monkey. *J. Comp. Neurol.*, 358, 119–141.
- Shink, E., Bevan, M.D., Bolam, J.P., Smith, Y., 1996. The subthalamic nucleus and the external pallidum: two tightly interconnected structures that control the output of the basal ganglia in the monkey. *Neuroscience*, 73, 335–357.
- Sidibé, M., Smith, Y., 1996. Differential synaptic innervation of striatofugal neurones projecting to the internal or external segments of the globus pallidus by thalamic afferents in the squirrel monkey. *J. Comp. Neurol.*, 365, 445–465.

- Smith, Y., Lavoie, B., Dumas, J., Parent, A., 1989. Evidence for a distinct nigropallidal dopaminergic projection in the squirrel monkey. *Brain Res.*, 482, 381–386.
- Smith, Y., Bolam, J.P., Von Krosigk, M., 1990a. Topographical and synaptic organization of the GABA-containing pallidsubthalamic projection in the rat. *Eur. J. Neurosci.*, 2, 500–511.
- Smith, Y., Hazrati, L.-N., Parent, A., 1990b. Efferent projections of the subthalamic nucleus in the squirrel monkey as studied by the PHA-L anterograde tracing method. *J. Comp. Neurol.*, 294, 306–323.
- Smith, Y., Wichmann, T., DeLong, M.R., 1994. Synaptic innervation of neurones in the internal pallidal segment by the subthalamic nucleus and the external pallidum in monkeys. *J. Comp. Neurol.*, 343, 297–318.
- Stanford, I.M., Cooper, A.J., 1999. Presynaptic  $\mu$  and  $\delta$  opioid receptor modulation of GABA<sub>A</sub> IPSCs in the rat globus pallidus *in vitro*. *J. Neurosci.*, 19, 4796–4803.
- Steiner, H., Gerfen, C.R., 1998. Role of dynorphin and enkephalin in the regulation of striatal output pathways and behavior. *Exp. Brain Res.*, 123, 60–76.
- Steriade, M., 2001. The GABAergic reticular nucleus: A preferential target of corticothalamic projections. *Proc. Natl. Acad. Sci. USA*, 98, 3625–3627.
- Steriade, M., Domich, L., Oakson, G., 1986. Reticularis thalami neurons revisited: activity changes during shifts in states of vigilance. *J. Neurosci.*, 6, 68–81.
- Steriade, M., Timofeev, I., Dürmüller, N., Grenier, F., 1998. Dynamic properties of corticothalamic neurons and local cortical interneurons generating fast rhythmic (30–40 Hz) spike bursts. *J. Neurophysiol.*, 79, 483–490.
- Steriade, M., Timofeev, I., Grenier, F., 2001. Natural waking and sleep states: a view from inside neocortical neurons. *J. Neurophysiol.*, 85, 1969–1985.
- Sterio, D., Berić, A., Dogali, M., Fazzini, E., Alfaro, G., Devinsky, O., 1994. Neurophysiological properties of pallidal neurons in Parkinson's disease. *Ann. Neurol.*, 35, 586–591.
- Strauss, U., Zhou, F.-W., Henning, J., Battfeld, A., Wree, A., Köhling, R., Haas, S.J.-P., Benicke, R., Rolfs, A., Gimsa, U., 2008. Increasing extracellular potassium results in subthalamic neuron activity resembling that seen in a 6-hydroxydopamine lesion. *J. Neurophysiol.*, 99, 2902–2915.
- Strick, P.L., Dum, R.P., Picard, N., 1995. Macro-organization of the circuits connecting the basal ganglia with the cortical motor areas. In: Houk, J., Davis, J., Beiser, D. (Eds.), *Models of Information Processing in the Basal Ganglia*. MIT Press, Cambridge, Massachusetts, pp. 117–130.
- Surmeier, D.J., Eberwine, J., Wilson, C.J., Cao, Y., Stefani, A., Kitai, S.T., 1992. Dopamine receptor subtypes colocalize in rat striatonigral neurons. *Proc. Natl. Acad. Sci. USA*, 89, 10178–10182.
- Surmeier, D.J., Song, W.-J., Yan, Z., 1996. Coordinated expression of dopamine receptors in neostriatal medium spiny neurons. *J. Neurosci.*, 16, 6579–6591.
- Swerdlow, N.R., Koob, G.F., 1987. Dopamine, schizophrenia, mania and depression – toward a unified hypothesis of cortico-striato-pallido-thalamic function. *Behav. Brain Sci.*, 10, 197–207.
- Taverna, S., van Dongen, Y.C., Groenewegen, H.J., Pennartz, C.M.A., 2004. Direct physiological evidence for synaptic connectivity between medium-sized spiny neurons in rat nucleus accumbens *in situ*. *J. Neurophysiol.*, 91, 1111–1121.
- Terman, D., Rubin, J.E., Yew, A.C., Wilson, C.J., 2002. Activity patterns in a model for the subthalamopallidal network of the basal ganglia. *J. Neurosci.*, 22, 2963–2976.

- Thomson, A.M., 1997. Activity-dependent properties of synaptic transmission at two classes of connections made by rat neocortical pyramidal axons in vitro. *J. Physiol.*, 502, 131–147.
- Thurley, K., Senn, W., Lüscher, H.-R., 2008. Dopamine increases the gain of the input-output response of rat prefrontal pyramidal neurons. *J. Neurophysiol.*, 99, 2985–2997.
- Toan, D.L., Schultz, W., 1985. Responses of rat pallidum cells to cortex stimulation and effects of altered dopaminergic activity. *Neuroscience*, 15, 683–694.
- Tseng, K.Y., Kasanetz, F., Kargieman, L., Riquelme, L.A., Murer, M.G., 2001. Cortical slow oscillatory activity is reflected in the membrane potential and spike trains of striatal neurons in rats with chronic nigrostriatal lesions. *J. Neurosci.*, 21, 6430–6439.
- Turner, J.P., Salt, T.E., 1998. Characterization of sensory and corticothalamic excitatory inputs to rat thalamocortical neurones in vitro. *J. Physiol.*, 510, 829–843.
- Umemiya, M., Raymond, L.A., 1997. Dopaminergic modulation of excitatory postsynaptic currents in rat neostriatal neurons. *J. Neurophysiol.*, 78, 1248–1255.
- Ungerstedt, U., 1968. 6-hydroxy-dopamine induced degeneration of central monoamine neurons. *Eur. J. Pharmacol.*, 5, 107–110.
- Uno, M., Ozawa, N., Yoshida, M., 1978. The mode of pallido-thalamic transmission investigated with intracellular recording from cat thalamus. *Exp. Brain Res.*, 33, 493–507.
- Van Albada, S.J., Gray, R.T., Drysdale, P.M., Robinson, P.A. Mean-field modeling of the basal ganglia-thalamocortical system. II. Dynamics of electrophysiological changes in Parkinson's disease. *J. Theor. Biol.*, 257, 664–688.
- Voloshin, M.Y., Prokopenko, V.F., 1978. Neuronal responses of the reticular and anterior ventral thalamic nuclei to stimulation of the thalamic ventrolateral nucleus and motor cortex. *Neurophysiology*, 10, 336–342.
- Walker, F.O., 2007. Huntington's disease. *Lancet*, 369, 218–228.
- Walters, J.R., Hu, D., Itoga, C.A., Parr-Brownlie, L.C., Bergstrom, D.A., 2007. Phase relationships support a role for coordinated activity in the indirect pathway in organizing slow oscillations in basal ganglia output after loss of dopamine. *Neuroscience*, 144, 762–776.
- Wannier, T.M.J., Maier, M.A., Hepp-Reymond, M.-C., 1991. Contrasting properties of monkey somatosensory and motor cortex neurons activated during the control of force in precision grip. *J. Neurophysiol.*, 65, 572–589.
- Waters, C.M., Peck, R., Rossor, M., Reynolds, G.P., Hunt, S.P., 1988. Immunocytochemical studies on the basal ganglia and substantia nigra in Parkinson's disease and Huntington's chorea. *Neuroscience*, 25, 419–438.
- Wichmann, T., Bergman, H., Starr, P.A., Subramanian, T., Watts, R.L., DeLong, M.R., 1999. Comparison of MPTP-induced changes in spontaneous neuronal discharge in the internal pallidal segment and in the substantia nigra pars reticulata in primates. *Exp. Brain Res.*, 125, 397–409.
- Williams, S.M., Goldman-Rakic, P.S., 1993. Characterization of the dopaminergic innervation of the primate cortex using a dopamine-specific antibody. *Cereb. Cortex*, 3, 199–222.
- Wilson, C.J., 1995. The contribution of cortical neurons to the firing pattern of striatal spiny neurons. In: Houk, J., Davis, J., Beiser, D. (Eds.). *Models of Information Processing in the Basal Ganglia*. MIT Press, Cambridge, Massachusetts, pp. 29–50.
- Wright, J.J., Liley, D.T.J., 1995. Simulation of electrocortical waves. *Biol. Cybern.*, 72, 347–356.
- Wu, J.-Y., Guan, L., Tsau, Y., 1999. Propagating activation during oscillations and evoked responses in neocortical slices. *J. Neurosci.*, 19, 5005–5015.

- Wu, Y., Richard, S., Parent, A., 2000. The organization of the striatal output system: a single-cell juxtacellular labeling study in the rat. *Neurosci. Res.*, 38, 49–62.
- Xu, W., Huang, X., Takagaki, K., Wu, J.-Y., 2007. Compression and reflection of visually evoked cortical waves. *Neuron*, 55, 119–129.
- Yelnik, J., 2002. Functional anatomy of the basal ganglia. *Mov. Disord.*, 17 (Suppl. 3), S15–S21.
- Yelnik, J., François, C., Percheron, G., Tandé, D., 1991. Morphological taxonomy of the neurons of the primate striatum. *J. Comp. Neurol.*, 313, 273–294.
- Yoshida, M., 1991. The neuronal mechanism underlying parkinsonism and dyskinesia: differential roles of the putamen and caudate nucleus. *Neurosci. Res.*, 12 (1), 31–40.
- Yoshida, S., Nambu, A., Jinnai, K., 1993. The distribution of the globus pallidus neurons with input from various cortical areas in the monkeys. *Brain. Res.*, 611, 170–174.
- Zhou, F.-M., Hablitz, J.J., 1999. Dopamine modulation of membrane and synaptic properties of interneurons in rat cerebral cortex. *J. Neurophysiol.*, 81, 967–976.
- Zhu, Z.T., Bartol, M., Shen, K.Z., Johnson, S.W., 2002. Excitatory effects of dopamine on subthalamic nucleus neurons: in vitro study of rats pretreated with 6-hydroxydopamine and levodopa. *Brain Res.*, 945, 31–40.
- Zweig, R.M., Jankel, W.R., Hedreen, J.C., Mayeux, R., Price, D.L., 1989. The pedunculopontine nucleus in Parkinson's disease. *Ann. Neurol.*, 26, 41–46.